Stem Cell Reports
Article

ISSCR

OPEN ACCESS

Detection of Retinal Pigment Epithelium-Specific Antibody in iPSC-Derived Retinal Pigment Epithelium Transplantation Models

Sunao Sugita,[1,*] Kenichi Makabe,[1] Shota Fujii,[1,2] Yuko Iwasaki,[1,3] Hiroyuki Kamao,[1,4] Takashi Shiina,[5] Kazumasa Ogasawara,[6] and Masayo Takahashi[1]

[1]Laboratory for Retinal Regeneration, Center for Developmental Biology, RIKEN, 2-2-3 Minatojima-minamimachi, Chuo-ku, Kobe 650-0047, Japan
[2]Department of Ophthalmology, Keio University School of Medicine, Tokyo, Japan
[3]Department of Ophthalmology & Visual Science, Tokyo Medical and Dental University Graduate School of Medicine and Dental Sciences, Tokyo, Japan
[4]Department of Ophthalmology, Kawasaki Medical School, Okayama, Japan
[5]Department of Molecular Life Science, Division of Basic Medical Science and Molecular Medicine, Tokai University School of Medicine, Kanagawa, Japan
[6]Department of Pathology, Shiga University of Medical Science, Ohtsu, Japan
*Correspondence: sunaoph@cdb.riken.jp
https://doi.org/10.1016/j.stemcr.2017.10.003

SUMMARY

Antibody-mediated rejection is characterized by donor-specific antibody produced by B cells. However, to our knowledge, B cell invasion and antibody in the inflamed retina after transplantation of retinal pigment epithelial (RPE) cells has not been reported. To determine if RPE transplantation could be performed using allografts, we established *in vivo* immune rejection models with induced pluripotent stem cell (iPSC)-RPE allografts and determined whether RPE-specific antibody could be detected in these models. We detected alloantibodies in the serum from recipient monkeys that had immune attacks in the retina in an immunofluorescent assay using the transplanted iPSC-RPE cells as the antigen. In addition to T cell and antigen-presenting cell immunity, peripheral blood cells and lymph nodes in animal models with allogeneic iPSC-RPE cells also had activated B cells, which were probably secreting alloantibodies. Using serum and transplanted cells, alloreactive antibody can be detected for the diagnosis of immune rejection after transplantation.

INTRODUCTION

Immune attacks occur after successful retinal transplantation and are a barrier to such transplantation, despite the existence of ocular immune privilege (Mochizuki et al., 2013; Streilein, 2003; Sugita, 2009). Corneal transplantation is not only the most frequently performed solid-organ transplantation in the world but it is also the most successful. In contrast, there is little trustworthy information available regarding immunological mechanisms in retinal transplantation. However, whether it is necessary to use retinal transplantation to treat severe retinal diseases is presently being reconsidered since stem cell transplantation is now one of the options for their treatment. We recently reported successful transplantation of retinal pigment epithelial (RPE) cells established from induced pluripotent stem cells (iPSCs) to treat a patient with age-related macular degeneration (AMD) (Mandai et al., 2017).

Over a decade ago, the first clinical trial for human retinal disorders used human allogeneic RPE cells; since these were allografts, the patients suffered immune rejection after surgery (Algvere, 1997; Algvere et al., 1999; Weisz et al., 1999). In another study, autografts of RPE cells were accepted by AMD patients after surgery (van Meurs et al., 2004). In addition, we recently reported that explanted iPSC-derived RPE cells (autografts) survived, and no immune inflammation occurred in the retina after transplantation (Mandai et al., 2017). In animal models using human fetal RPE cells (Sheng et al., 1995), which were xenografts, the monkey or rabbit models displayed immune rejection and the graft did not survive. Thus, RPE cells serve as targets of immune rejection after allogeneic transplantation.

Graft rejection after transplantation has generally been considered primarily as a manifestation of cellular immune responses, especially of T cells. However, a role for antibodies produced by B cells has been suspected in cell/tissue transplantation, and antibody-mediated rejection has emerged as an important cause of graft failure (Berry et al., 2013; Colvin and Smith, 2005; Wallace et al., 2014). Alloantibody-medicated rejection has been widely recognized in organ transplantation (Berry et al., 2013; Wallace et al., 2014), and antibody-mediated rejection has been characterized by donor-specific antibodies, particularly anti-human leukocyte antigen (HLA) antibodies. However, antibody-mediated rejection may occur as a result of other donor-specific antibodies (Colvin and Smith, 2005). In a corneal study, although B cells and alloantibodies did not seem to be necessary for corneal graft rejection (Goslings et al., 1999), these antibodies could produce extensive injury to corneal allografts in mouse models (Hegde et al., 2002). We recently reported that iPSC-derived RPE cells invoked immune responses in the retina of major histocompatibility complex (MHC)-mismatched donors after transplantation in animal models. These data indicated that there are inflammatory immune rejections around RPE grafts and retinal tissue damage, together with inflammatory cell invasion, T cells, retinal microglia, and antigen-presenting cells (APCs) in the retina,

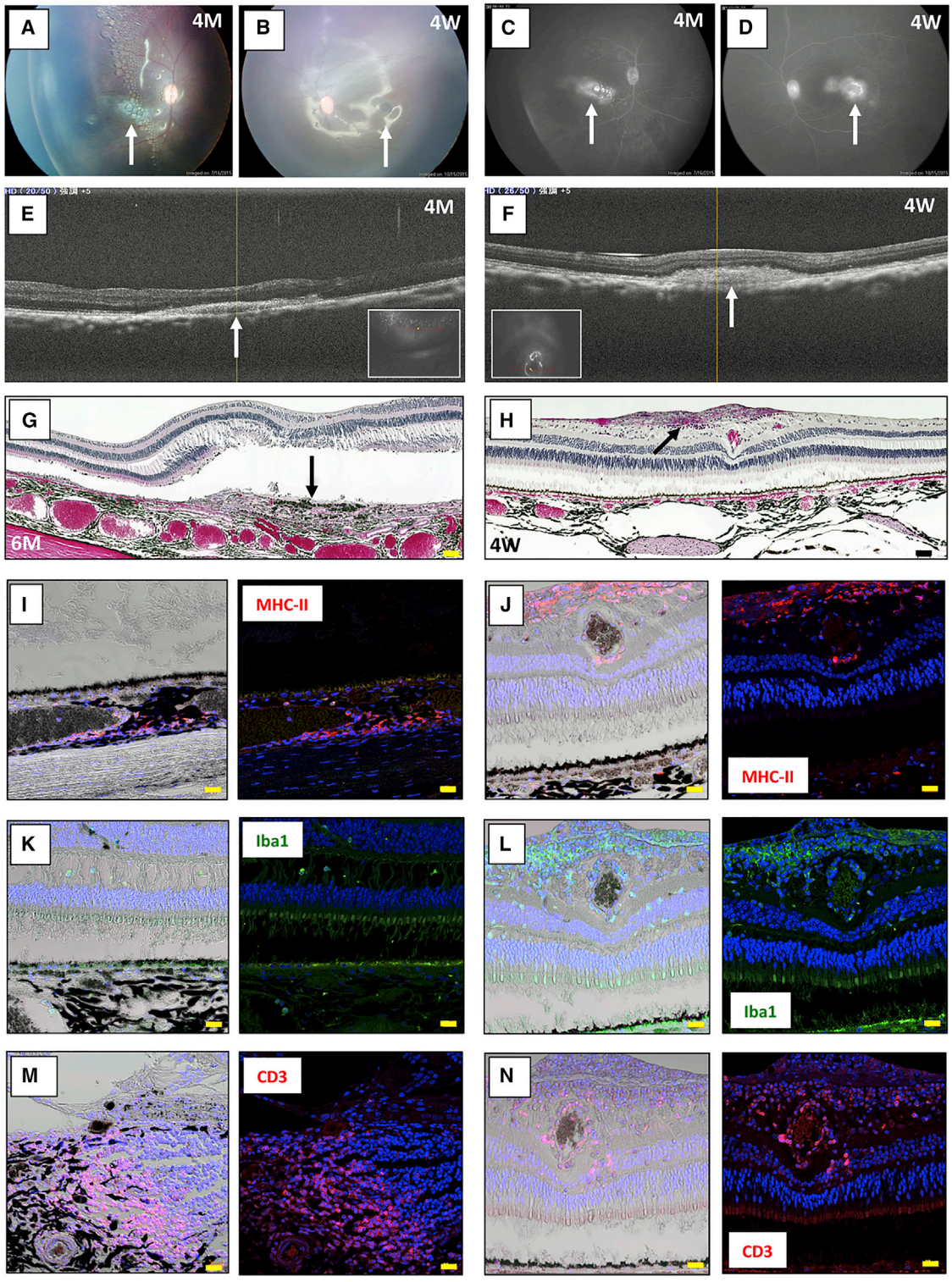

Figure 1. Allogeneic Transplantation of an iPSC-RPE Cell Sheet into the Subretinal Space of an MHC Haplotype-Mismatched Immune Rejection Animal Model

(A–F) Transplantation of the 46a iPS-RPE cell sheet into the subretinal space of a TLHM1 monkey (allografts, both eyes). The right eye at 16 weeks (4 months [4M]) and left eye at 4 weeks (4W) after surgery are shown. Color photographs of the fundus (A, right eye; B, left eye)

(legend continued on next page)

subretinal space, and choroid (Sugita et al., 2016a). However, to our knowledge, there has been no report of the existence of B cells or alloantibodies around retinal allografts after transplantation.

The purpose of this study was therefore to investigate whether allogeneic RPE cells derived from iPSCs (iPS-RPE cells) invoke immune attacks including B cell invasion in the retina. We used an *in vivo* animal model with monkey iPS-RPE cells as allografts. We further examined whether there is B cell activation in blood cells and lymph nodes of these animal models with allogeneic iPS-RPE cells. In addition, we determined whether alloantibodies in the serum collected from monkey graft recipients could be detected in an immunofluorescent assay using the transplanted iPS-RPE cells as antigen.

RESULTS

Allogeneic iPS-RPE Cells from Monkey iPSCs Are Immunogenic and Invoke Inflammatory Cell Infiltration in the Retina in *In Vivo* Animal Models

In the present study, we used six *in vivo* monkey animal models as operated monkeys and two normal monkeys as controls. We first transplanted allogeneic iPS-RPE cells into monkey eyes in MHC-mismatched donors (cynomolgus monkeys without immunosuppression). MHC profiles of the transplanted monkeys are shown in Table S1 and those of the monkey iPS-RPE cells are described in a previous report (Sugita et al., 2016a). Inflammation (=immune rejection) was evaluated by color photography of the fundus, fluorescein angiography (FA), and optical coherence tomography (OCT) after vitrectomy at 1, 2, 4, 8, 12, and 16 weeks and at 6 months after transplantation (Kamao et al., 2014; Sugita et al., 2016a).

There were signs of immune rejection in the allografts of the MHC-mismatched monkeys (46a iPS-RPE cell sheets into TLHM1 normal monkey eyes; Figure 1). For example, explanted RPE cell sheets exhibited a scar-like appearance (Figures 1A and 1B), and fluorescein leakage was detected in the sheet grafts in FA (Figures 1C and 1D). In addition, a retinal mass-like lesion around the graft was detected in OCT (Figures 1E and 1F). We also histologically examined whether the models transplanted with iPS-RPE cells had inflammatory cells by conducting H&E staining and inflammatory cell immunohistochemistry (IHC) of paraffin-embedded retinal sections. In IHC analysis, the retina in the TLHM1 monkey was stained with anti-MHC class II (MHC-II), ionized calcium-binding adapter molecule 1 (Iba1), and CD3 antibodies. In H&E staining, although the RPE sheet transplanted into the TLHM1 monkey was in the subretinal space, the sheet exhibited hypertrophic changes such as a mass (nodule) with infiltrating cells seen in the right eye (Figure 1G) and a mass of infiltrated cells in the retina of the left eye (Figure 1H), indicating immune rejection features in the allografts. The IHC analysis indicated that there were numerous MHC-II$^+$ cells (activated APCs; Figures 1I and 1J), Iba1$^+$ cells (amoeboid-type activated microglia; Figures 1K and 1L), and CD3$^+$ cells (T cells; Figures 1M and 1N) in the inflammatory lesions.

Similarly, in the case of another allograft transplantation (TLHM6 monkey; 46a iPS-RPE cell sheets into the right eye), signs of immune rejection of the graft in the retinas of both eyes were found in FA, OCT, H&E, and IHC analyses (Figure S1). Thus, as reported previously (Sugita et al., 2016a), there were signs of rejection of allogeneic iPSC-derived RPE cells in a normal monkey that had ocular inflammation after transplantation without immunosuppressive medication.

Animal Models with Allogeneic iPS-RPE Cells Have IgG and B Cell Infiltration in the Retina

We next examined whether the eyes of models transplanted with iPS-RPE cells have inflammatory B cells. We immunostained retinal sections with anti-immunoglobulin G (IgG), CD20, and/or CD40 antibodies. In the sections from a normal healthy monkey (without operation),

and fluorescein angiography (FA) (C, right eye; D, left eye) indicated inflammation (a scar-like sheet and also graft leakages in FA [arrows]). Optical coherence tomography (OCT) (E, right eye; F, left eye) showed cell infiltration (arrow) into the subretinal space. Inset in the OCT image indicates the fundus image.

(G) At 6 months, the right eye of the TLHM1 monkey was H&E-stained for histological interpretation. The RPE sheet was in the subretinal space; however, the sheet exhibited hypertrophic changes such as the appearance of a nodule (arrow) with inflammatory infiltrating cells in the eye. Scale bar, 50 μm.

(H–N) In H&E analysis, (H) the transplanted RPE sheet had disappeared from the subretinal space, and cell infiltration into the retina of the operated left eye was seen (arrow). Scale bar, 50 μm. Photographs of the retina in the right eye at 6 months are labeled with anti-MHC-II (I), Iba1 (K), or CD3 antibody (M) and co-stained for nuclei with DAPI. Left photographs, light microscopy; right photographs, immunofluorescence. Numerous MHC-II$^+$ cells were seen in the choroid, and amoeboid-type Iba1$^+$ cells were also seen in the retina. Many CD3$^+$ T cells had invaded into the inflammatory nodule. Scale bars, 20 μm. IHC analysis in the left eye at 4W indicated that numerous MHC-II$^+$ cells (J), amoeboid-type Iba1$^+$ cells (L), and CD3$^+$ T cells (N) had invaded into the retina. Nuclei in the right photographs were co-stained with DAPI. Scale bars, 20 μm.

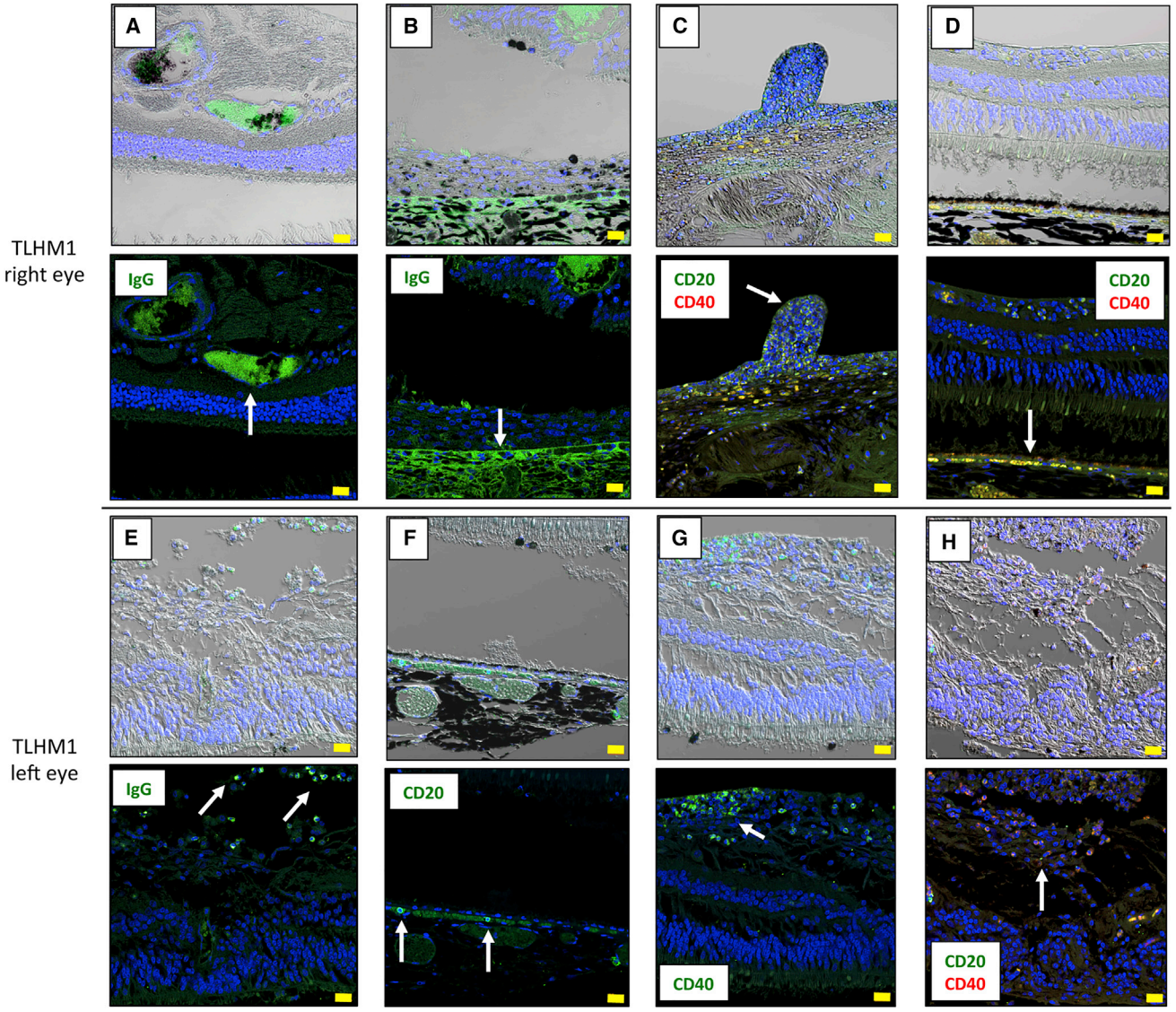

Figure 2. Immunohistochemistry for IgG and B Cells in a TLHM1 Rejection Monkey

Photomicrographs show labeling of the TLHM1 retina in monkeys grafted with iPS-RPE cell sheets into both eyes with anti-IgG, anti-CD20, and/or anti-CD40 antibodies. Cell nuclei were counterstained with DAPI (blue). Enhanced staining of IgG was seen around the iPS-RPE cell sheet graft (A, arrow) and host RPE layer (B, arrow) in the right eye. Many $CD20^+$ cells were seen in the retina, and $CD20^+/CD40^+$ double-positive cells (yellow, activated B cells) were also seen in the retinal nodules (C, arrow). These double-positive cells were also seen in the retina and under the host RPE layer (D, arrow). In the left eye, IgG^+ cells (probably B cells) were seen in the retina (E, arrows), and $CD20^+$ cells were also seen under the host RPE layer (F, arrows). In addition, many $CD40^+$ activated B cells had invaded into the retina (G, arrow), and $CD20^+/CD40^+$ double-positive cells were also seen in the retina (H, arrow). Scale bars, 20 μm.

there were no CD20- or CD40-positive cells in the retina, and, although there was weak staining of IgG in the choroid, there was no IgG staining in the retina (data not shown).

In contrast, in TLHM1 rejection monkey eyes, there was enhanced staining of IgG around the RPE grafts in the retina (Figure 2A) and host RPE layer (Figure 2B), as well as the presence of retinal infiltrating cells (probably B lymphocytes; Figure 2E) in the transplanted eyes. In addition, there were numerous $CD20^+$ cells (B cells; Figures 2C, 2D, 2F, and 2H) and $CD40^+$ cells (activated B cells; Figures 2C, 2D, 2G, and 2H) in the inflammatory lesions. Although there were no $CD20^+$ B cells and little IgG staining (Figure S2) throughout the retinal sections from the DrpZ17 monkey (MHC haplotype-matched), we did observe $CD20^+$ cells, $CD40^+$ cells, and IgG in IHC analysis in cases

of transplantation of another RPE allograft into the eye of MHC haplotype-mismatched TLHM6 (Figure S1) and S3-2 (Figure S2) monkeys. Importantly, there were numerous $CD20^+$ and $CD40^+$ B cells around iPS-RPE graft cells in the eye of TLHM6 monkeys (Figure S1).

Moreover, we also showed results for xenografts (human iPSC-derived RPE cells into K-189 monkey). In order to locate the immune attacks, we performed IHC staining for IgG, B cells (CD20), and T cells (CD3). Similar to the results of allografts, transplanted human iPS-RPE grafts were rejected, and the monkey had B cell invasion, as well as T cells, in the retina (Figure S3). These results suggested that there are alloantibody-mediated immune attacks against iPSC-derived RPE cells (both allografts and xenografts) in the retina, in addition to the presence of T cells and APC inflammation (Sugita et al., 2016a).

Lymph Nodes in Animal Models with Allogeneic iPS-RPE Cells Have B Cell Invasion

We next evaluated B cells in the lymph nodes (LNs) of monkeys after iPS-RPE transplantation. After monkey sacrifice, we collected LN tissues from the neck and ear of S3-2 and DrpZ17 monkeys. The results of transplantation of S3-2 (MHC haplotype-mismatched; rejection in eyes) and DrpZ17 (MHC haplotype-matched; no rejection in eyes) monkeys were previously reported (Sugita et al., 2016a). We then performed H&E staining of LN sections and conducted IHC for $CD20^+$ B cells. Numerous lymphoid cells were observed in the LNs from the neck of the S3-2 monkey, and the LNs were actually swollen (Figure 3A). In contrast, although the LNs from the neck of the DrpZ17 monkey also included lymphoid cells, these neck LNs were not swollen and appeared to be of normal size (Figure 3B). Similarly, we found lymphoid cells in the ear LNs in the S3-2 monkey (Figure 3C) but not in those of the DrpZ17 monkey (Figure 3D). IHC analysis indicated that there were numerous $CD20^+$ B cells in the neck (Figure 3E) and ear (Figure 3F) LNs of the S3-2 monkey; however, there were little (Figure 3G) or no (Figure 3H) B cells in the LNs from the DrpZ17 monkey. Similarly, by using fluorescence-activated cell sorting (FACS) analysis, we found that there were increased B cells in the LN tissues of the TLHM6 rejection monkey compared with the peripheral blood mononuclear cells (PBMCs) from the TLHM6 or normal monkey (Figure S4). These results indicated that *in vivo* animal models with allogeneic iPS-RPE cells have B cell infiltration in the draining LNs, as well as in intraocular tissues such as the retina.

B Cells in PBMCs Respond to Allogeneic iPSC-Derived RPE Cells *In Vitro*

We next examined whether B cells in the periphery could respond to allogeneic iPS-RPE cells and whether B cells exposed to the RPE cells could be activated *in vitro*. Mixed lymphocyte reaction (MLR) assays were conducted as described in our previous reports (Sugita et al., 2016a, 2016b). In the MLR assays using PBMCs prepared from TLHM6 monkeys, fresh PBMCs prepared at 8 weeks after operation proliferated when co-cultured with allogeneic iPS-RPE cells (Figure 4A), e.g., $CD4^+$ cells (helper T cells), $CD8^+$ cells (cytotoxic T cells), $CD20^+$ cells (B cells), and $CD56^+$ cells (NK/NKT cells) in PBMCs showed higher proliferation in the presence, than the in absence, of RPE cells. The same PBMCs cultured with allogeneic monkey B cell lines (B95-8) as a positive control showed high proliferation (data not shown). Moreover, $CD20^+$ B cells in PBMCs and LN tissues prepared from TLHM6 monkeys at 8 weeks post operation that were exposed to iPS-RPE cells highly expressed MHC-II and CD86 (B7-2) co-stimulatory molecules compared with $CD20^+$ B cells in PBMCs only (Figure 4B) or LN cells only (Figure 4C) without RPE cells. In contrast, $CD20^+$ B cells in PBMCs from a K-254 normal monkey failed to be activated by the iPS-RPE cells *in vitro* (Figure 4D). These data suggested that memory-activated B cells against transplanted iPS-RPE cells may exist and circulate in the periphery of the monkey with the immune attack.

B Cells Fail to Respond to Allogeneic iPSC-Derived RPE Cells in the Presence of Medication

We next examined the effect of some suppressive medications in the *in vitro* RPE-PBMC MLR assay. For this purpose, we chose cyclosporin A, triamcinolone acetonide, betamethasone, and prednisolone because we generally use these drugs for patients with intraocular inflammatory disorders in Japan. All of these medications suppressed the PBMC response to allogeneic iPS-RPE cells using PBMCs prepared from TLHM6 monkeys at 12 weeks post operation (Figure 5A). However, these medications showed different efficacies; e.g., triamcinolone greatly suppressed T and B cell responses in PBMCs from a TLHM6 transplanted monkey to allogeneic iPS-RPE cells, whereas betamethasone showed poor efficacy (Figure 5A).

We confirmed the effect of triamcinolone in the *in vitro* RPE-PBMC MLR assay using blood cells from a pre-operation TLHM15 monkey. As shown in Figure 5B, triamcinolone and other medications such as cyclosporin A, betamethasone, and prednisolone suppressed the PBMC response to allogeneic iPS-RPE cells. Thus, T cells ($CD4^+$ and $CD8^+$) and B cells in PBMCs responded to allogeneic iPS-RPE cells, while triamcinolone greatly suppressed these lymphocyte responses. We therefore chose triamcinolone to control ocular inflammation after allogeneic iPS-RPE cell transplantation in subsequent experiments.

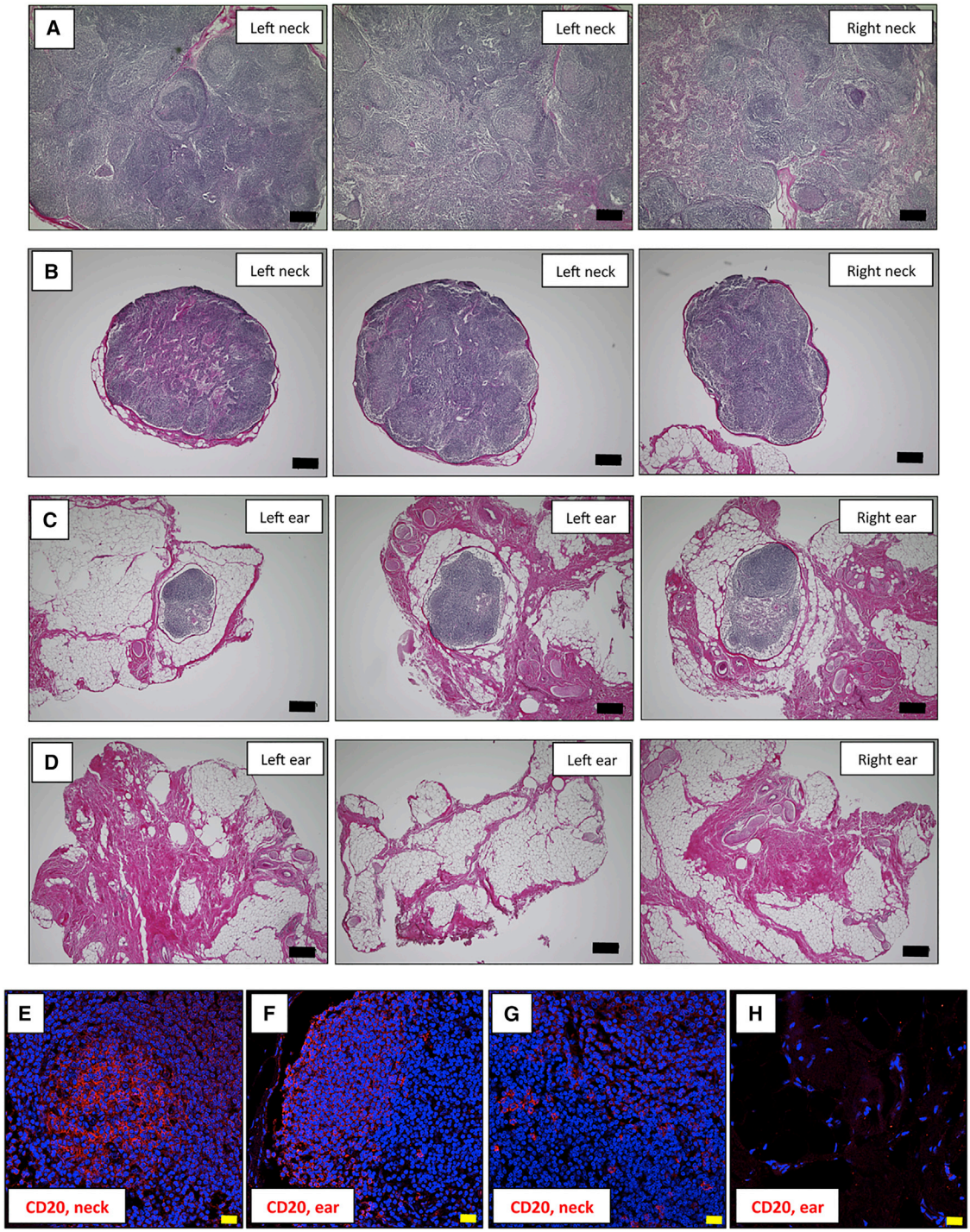

Figure 3. Immunohistochemistry of the Lymph Nodes (LN) in S3-2 and DrpZ17 Monkeys

H&E-stained LN tissues of an S3-2 rejection monkey (MHC haplotype-mismatched allograft; 1121A1 iPS-RPE sheet) or a DrpZ17 non-rejection monkey (MHC haplotype-matched allograft; 1121A1 iPS-RPE sheet) at 6 months after iPS-RPE transplantation are shown for histological interpretation.

(A–D) S3-2 neck LNs (A), DrpZ17 neck LNs (B), S3-2 ear LNs (C), and DrpZ17 ear LNs (D). Scale bars, 200 μm.

(E–H) Photomicrographs show IHC labeling of S3-2 or DrpZ17 monkey LN tissues for CD20. Nuclei are co-stained with DAPI (blue). Whereas many $CD20^+$ cells (E and F) had invaded the swollen LN tissues in the neck of the S3-2 monkey, little (G) or no (H) $CD20^+$ cells had invaded the non-swollen LN tissues in the DrpZ17 monkey. Scale bars, 20 μm.

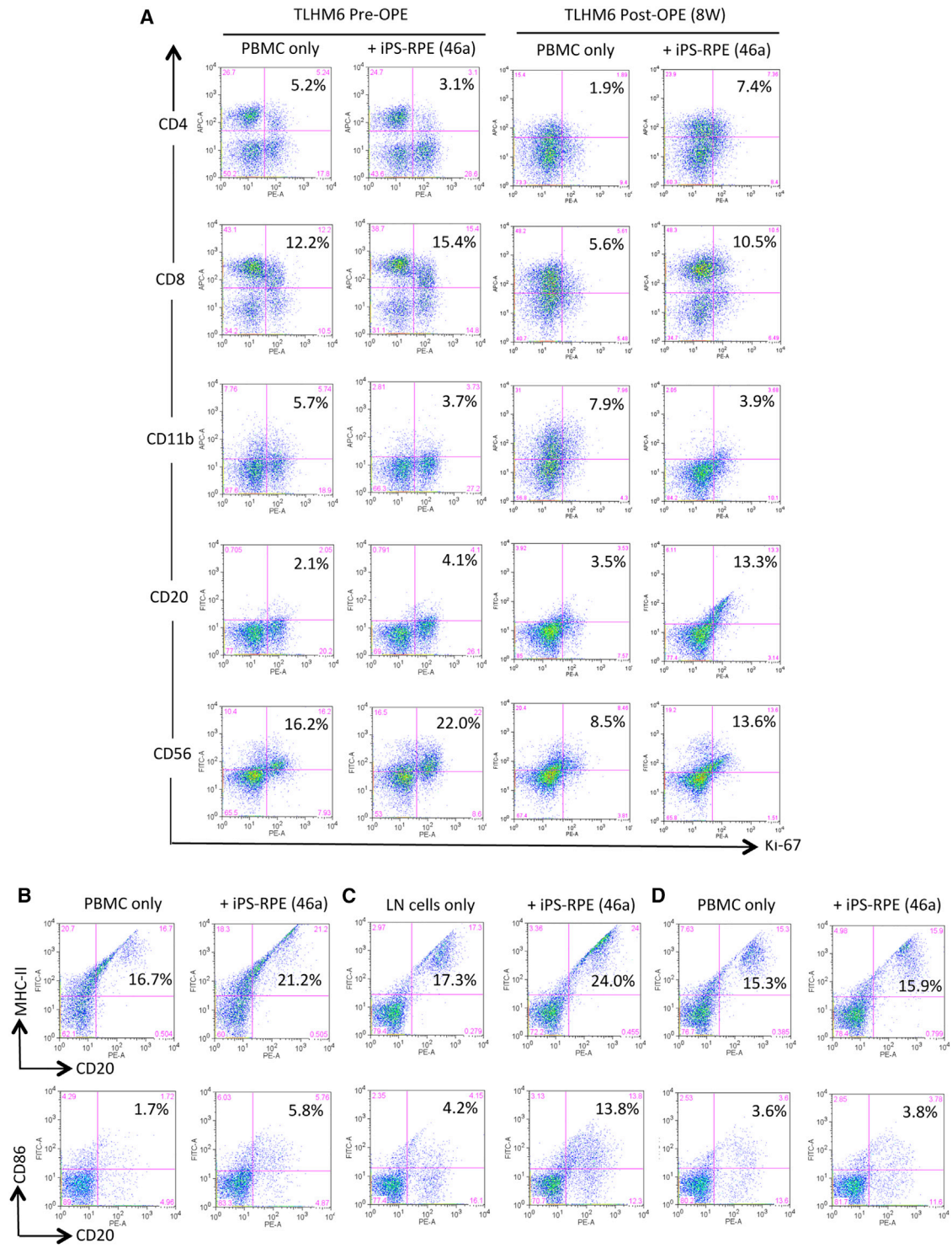

Figure 4. Mixed Lymphocyte Reaction Assays with PBMCs from the TLHM6 Monkey plus Transplanted iPSC-derived RPE Cells

(A) To evaluate the PBMC-RPE MLR assay using allogeneic iPS-RPE cells, fresh PBMCs (2×10^6 cells/well) prepared from a TLHM6 monkey at pre-operation (pre-OPE) or at 8 weeks post-OPE were cultured with 46a iPS-RPE cells for 96 hr. Before the assay, the RPE cells were irradiated (20 Gy), and 1×10^4 cells were cultured in a 24-well plate. Following the assay, the PBMCs were stained with anti-CD4, anti-CD8, anti-CD11b, anti-CD20, anti-CD56, or anti-Ki-67 antibody (plus each isotype control antibody) at 4°C for 30 min and then analyzed using

(legend continued on next page)

Efficacy of Local Steroid Injection for Prevention of Immune Rejection of Allogeneic iPS-RPE Cells in an *In Vivo* Animal Model

We next transplanted allogeneic iPS-RPE cells into the eye of an MHC haplotype-mismatched monkey donor (TLHM15) together with intravitreal triamcinolone acetonide (IVTA) and sub-Tenon triamcinolone acetonide (STTA). We performed IVTA injection on day 0 (operation day) and then performed STTA injection 4 weeks after surgery.

In the evaluation of the graft, there were no rejection signs around the RPE graft, including histological retinal findings (Figures S5A–S5D). In IHC analysis, there was no enhanced staining of IgG (Figure S5E) in the retina or RPE layer, and there were no $CD20^+$ (Figure S5G) or $CD40^+$ (Figures S5F and S5G) cells throughout the section.

Compared with the results obtained in the RPE-PBMC MLR assay using PBMCs from the TLHM6 monkey (see Figure 4), proliferation of PBMCs from the TLHM15 monkey in this assay was poor, including B cell proliferation, even if PBMCs were collected after transplantation (Figure S5H). Moreover, the expression of MHC-II and CD86 molecules was not upregulated even when $CD20^+$ B cells in PBMCs from the TLHM15 monkey were exposed to iPS-RPE cells (Figure S5I). Thus, although allogeneic iPS-RPE cells have B cell-mediated inflammation in the retina after transplantation, there were no rejection signs, including no B cell filtration into the retina, in allogeneic iPS-RPE explanted animals when IVTA/STTA injection was performed.

Detection of RPE-Specific Antibody in iPSC-RPE Transplanted Animal Models

Thus far, the results from *in vivo* and *in vitro* studies demonstrated that B cells, as well as T cells and APCs, play an important role in the inflammatory processes in iPS-RPE cell allografts after transplantation. Therefore, as a final step, we examined whether iPS-RPE cell transplanted monkeys had RPE-specific antibody (RSA) in the serum. For this assay, we collected the sera from several operated monkeys and prepared explanted graft iPS-RPE cells. After RPE cell fixation, we determined whether antibodies present in the serum could detect RPE cells using IHC. The iPS-RPE cells (46a RPE cells or 1121A1 RPE cells) were clearly much more strongly stained with the sera from TLHM1 (Figure 6A) and S3-2 (Figure 6C) monkeys that had immune attacks after transplantation compared with the staining of the serum from a normal K-151 monkey (Figure 6D). Conversely, the sera from TLHM15 monkeys that did not have immune attacks because of steroid injection failed to stain the RPE cells (Figure 6B). Other sera (taken at 1, 2, 4, 8, and 12 weeks after surgery) from TLHM15 monkeys also gave similar results, i.e., there was no RPE cell staining (data not shown). Similar results were also obtained using the serum from a DrpZ17 monkey that was transplanted with iPS-RPE cells (Figure S6). These results suggested that the transplanted monkeys with an immune attack may have alloreactive RPE-specific antibodies in their sera.

We also regularly collected and tested the sera (0, 1, 4, 6, 8, 12, and 16 weeks) from TLHM6 monkeys after transplantation. Although the transplanted RPE cells did not stain with the serum collected at 0, 1, or 4 weeks, the cells were strongly stained with the serum collected at 6 weeks (Figure 7A). Interestingly, the serum collected at 8 or 12 weeks did not stain the RPE cells, whereas the serum that was collected at 16 weeks, which was after the second operation for the left eye, clearly stained the RPE cells. When the mean fluorescence intensity in confocal microscopy was compared, the mean fluorescence intensity of the staining of the serum collected at 6 or 16 weeks was significantly increased compared with that of the control serum (0 weeks, before transplantation; Figure 7B). However, the intensity of the staining of the serum collected at 8 or 12 weeks was not increased, which indicates that the RPE cells were not stained with these sera. These results imply that the transplanted animal may have an eye-specific systemic immunosuppression such as an anterior chamber-associated immune deviation (ACAID) (Streilein et al., 2002; Wilbanks and Streilein, 1990) because the graft RPE cells were recognized by immune cells as allografts.

Conversely, throughout the evaluation period, no RPE staining was obtained using the serum from a DrpZ17 monkey with MHC homozygote iPS-RPE cells (Figure 7B). Moreover, the sera from animals with an immune attack failed to stain the RPE cells if the cells were pretreated with both anti-MHC class I and class II blocking antibodies (Figure 7C). These results suggested that the alloantibodies might include MHC (HLA)-specific antibodies.

DISCUSSION

In this study, we demonstrated that there were rejection signs in transplants of allogeneic iPS-RPE cells into MHC

flow cytometry. Compared with the PBMCs pre-OPE, all cell types in the PBMCs at post-OPE, except for $CD11b^+$ cells, had greatly proliferated after co-culture with allogeneic iPS-RPE cells. Numbers (%) in the histogram indicate double-positive cells (e.g., $CD4^+/Ki\text{-}67^+$).
(B–D) Expression of MHC class II (MHC-II) and CD86 (B7-2) co-stimulatory molecules on B cells exposed to iPS-RPE cells. PBMCs or LN cells in the presence of iPS-RPE cells were stained with anti-MHC-II, anti-CD86, and anti-CD20 antibodies and analyzed using flow cytometry. (B) TLHM6 PBMCs (post-OPE, 8W), (C) TLHM6 LN cells (post-OPE, 16W), and (D) K-254 PBMCs (normal control). Numbers (%) in the histogram indicate double-positive cells (e.g., $CD20^+/MHC\text{-}II^+$).

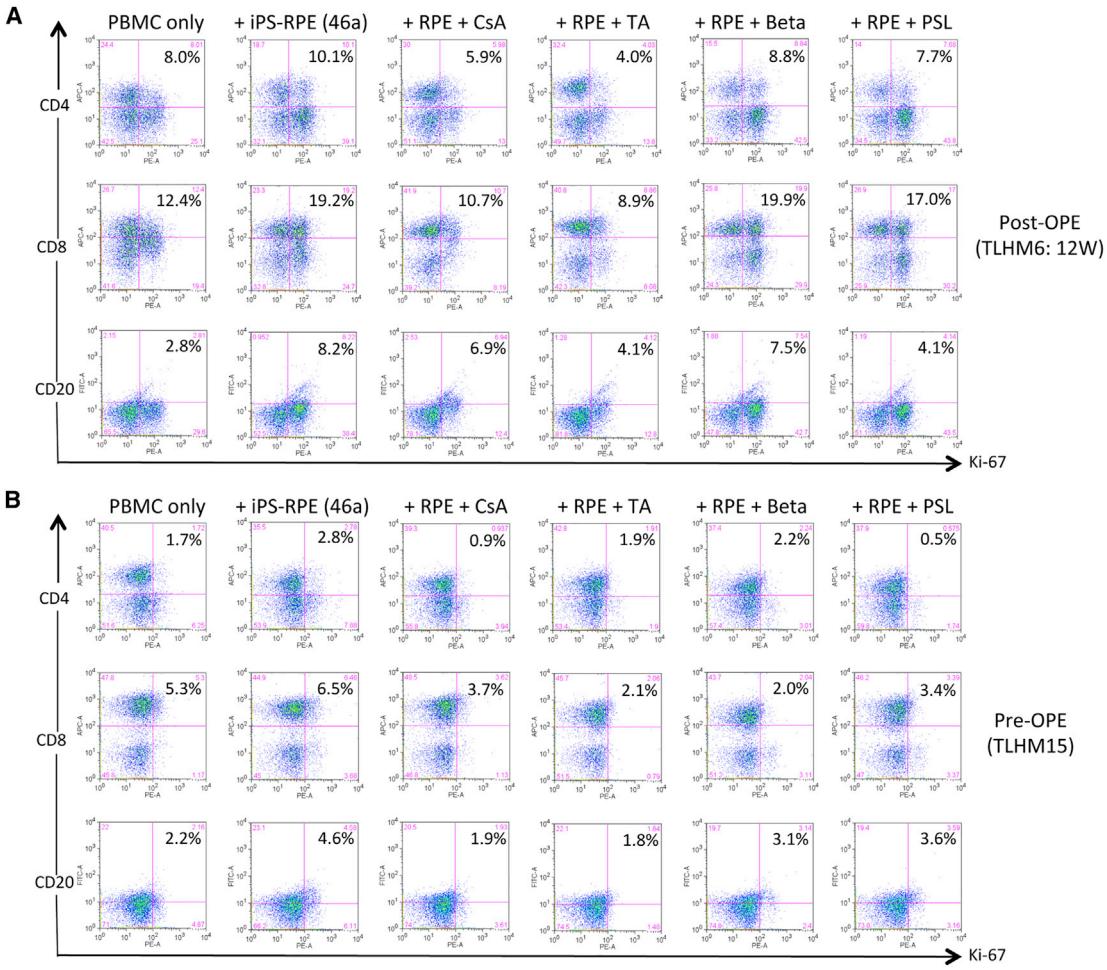

Figure 5. MLR Assay with Monkey PBMCs and Allogeneic iPS-RPE Cells in the Presence of Medication

Following PBMC-RPE MLR assay plus medication *in vitro*, $CD4^+$/Ki-67^+ (proliferated helper T cells), $CD8^+$/Ki-67^+ (proliferated cytotoxic T cells), and $CD20^+$/Ki-67^+ (proliferated B cells) cells were evaluated using flow cytometry. Compared with PBMCs from the TLHM6 monkey at 12 weeks (12W) post operation (post-OPE; A) or with PBMCs from the TLHM15 monkey (pre-OPE; B) incubated with 46a RPE cells, none of the cell types of PBMCs proliferated in the presence of medication such as cyclosporin A (CsA), triamcinolone (TA), betamethasone (Beta), or prednisolone (PSL). Numbers (%) in the histogram indicate double-positive cells (e.g., $CD4^+$/Ki-67^+).

haplotype-mismatched monkey eyes; namely, there was ocular inflammation after transplantation. Transplantation of allogeneic iPS-RPE cells resulted in alloantibody-mediated immune attacks in the retina, in addition to T cell and APC immunity. Importantly, we found enhanced staining of IgG around transplanted RPE grafts in the retina together with B cell invasion. Moreover, transplantation of human iPS-RPE cells (xenografts) resulted in immune attacks in the retina together with B cell invasion. The *in vivo* animal models with allogeneic iPS-RPE cells had B cell infiltration in the draining LNs as well as in the retina. In the *in vitro* RPE-PBMC MLR assay, B cells in PBMCs proliferated when co-cultured with allogeneic iPS-RPE cells. The B cells in PBMCs or in LN tissues that were exposed to iPS-RPE cells strongly expressed MHC class II and CD86 co-stimulatory molecules. However, there were no rejection signs and no B cell invasion in the retina of the RPE grafts if local steroid administration was performed. Importantly, we detected RSA in the monkeys that had an immune attack when we conducted an immunofluorescent assay to detect alloantibodies using transplanted RPE cells and the sera collected from the recipient monkeys. Moreover, the timing of B cell invasion (CD20/CD40) in the retina and detection of RSA in the sera from transplanted monkeys was the same.

Consistent with our previous report (Sugita et al., 2016a), there were rejection features, i.e., ocular inflammation including T cells and APCs (retinal microglia and macrophages in the choroid) following transplantation of allogeneic iPS-RPE cells into MHC haplotype-mismatched normal monkey eyes. The allogeneic iPS-RPE cells invoked

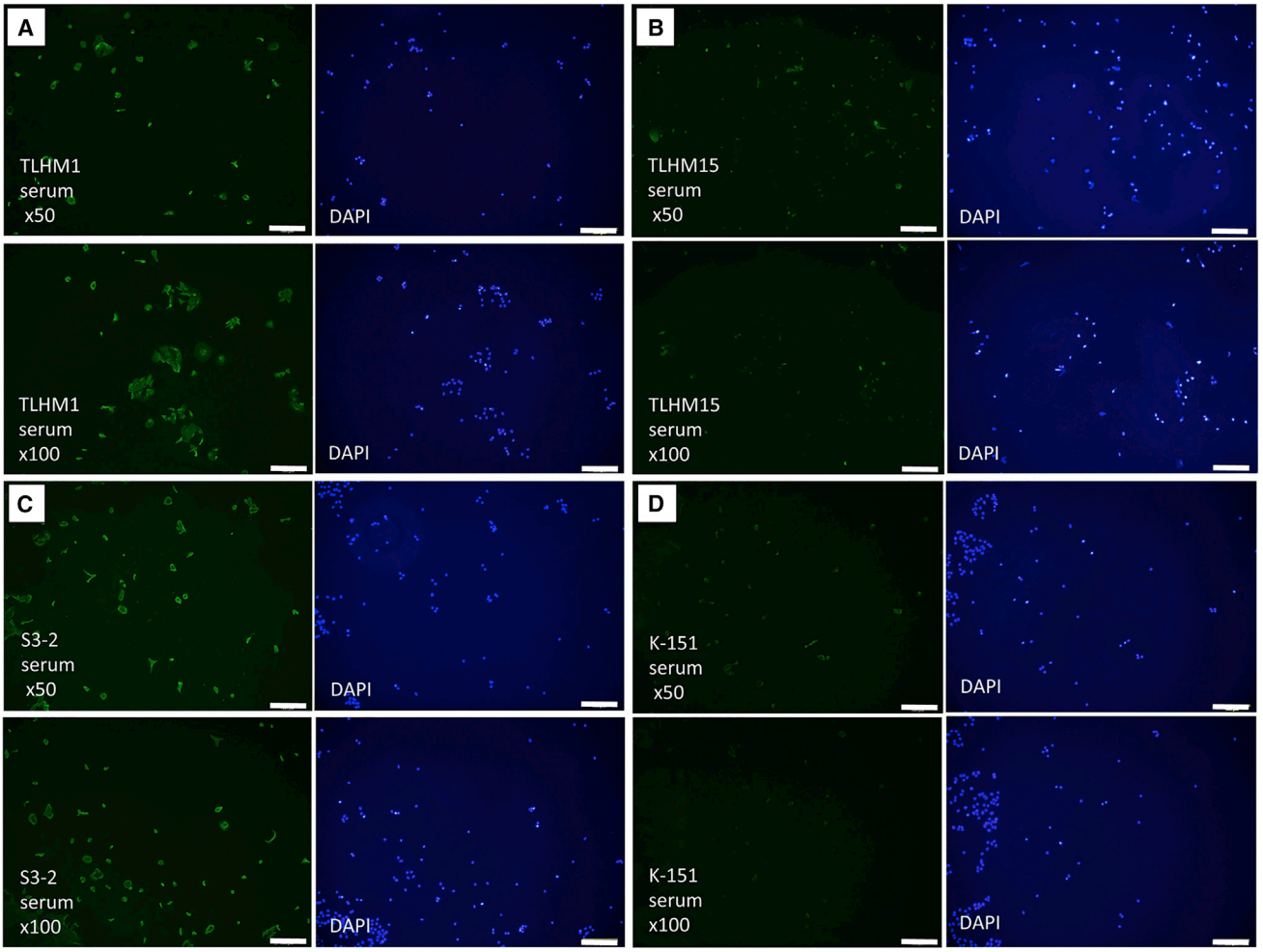

Figure 6. Detection of RPE-Specific Antibody in iPSC-RPE Cell Transplanted Animal Models

The sera from several operated monkeys (all 12 weeks after surgery) were collected, and transplanted iPS-RPE cells were prepared. After RPE cell fixation, immunohistochemistry was performed for RSA detection using the diluted sera. Nuclei were counterstained with DAPI. (A–D) 46a RPE cells + serum from a TLHM1 monkey, (B) 46a RPE cells + serum from a TLHM15 monkey that received injection into the eye, (C) 1121A1 RPE cells + serum from an S3-2 monkey, and (D) 46a RPE cells + serum from a normal K-151 monkey. Scale bars, 200 μm.

T cell- and APC-mediated immune rejection in the retina, and ultimately the RPE grafts did not survive. As shown in this study, *in vivo* monkey models transplanted with allogeneic iPS-RPE cells had B cell invasion ($CD20^+$ and/or $CD40^+$ cells) in the retina and enhanced IgG staining (probably produced by infiltrating B cells in the retina) around the RPE grafts. In addition, we found numerous MHC class II-positive cells in the retina and choroid in immune attack eyes, suggesting that these inflammatory MHC class II-positive cells may include B cells and macrophages. Moreover, we could not find intraocular B cells ($CD20^+$ and/or $CD40^+$) in retinal sections even in those from some immune attack monkeys (data not shown). Our findings suggest that B cells may disappear from the local space after (or during) the end of inflammatory events.

Conversely, the eyes in MHC haplotype-matched monkeys did not have immune attacks, consistent with a previous study (Sugita et al., 2016a). They had no B cell invasion, and the iPS-RPE cell grafts ultimately survived in the subretinal space. In addition, in iPS-RPE allografts of a monkey that received IVTA injection, there was no enhanced staining of IgG in the retina and RPE layer, and no B cells were detected in IHC staining of retinal sections, indicating that there was no immune attack. Thus, retinal inflammation may be controlled in MHC haplotype-matched retinal patients and/or by local steroid administration.

After transplantation with allografts, recipient T and B cells express receptors on their surface for antigens, and these receptors recognize transplantation antigens on the allografts. Upon recognition, these cells become activated,

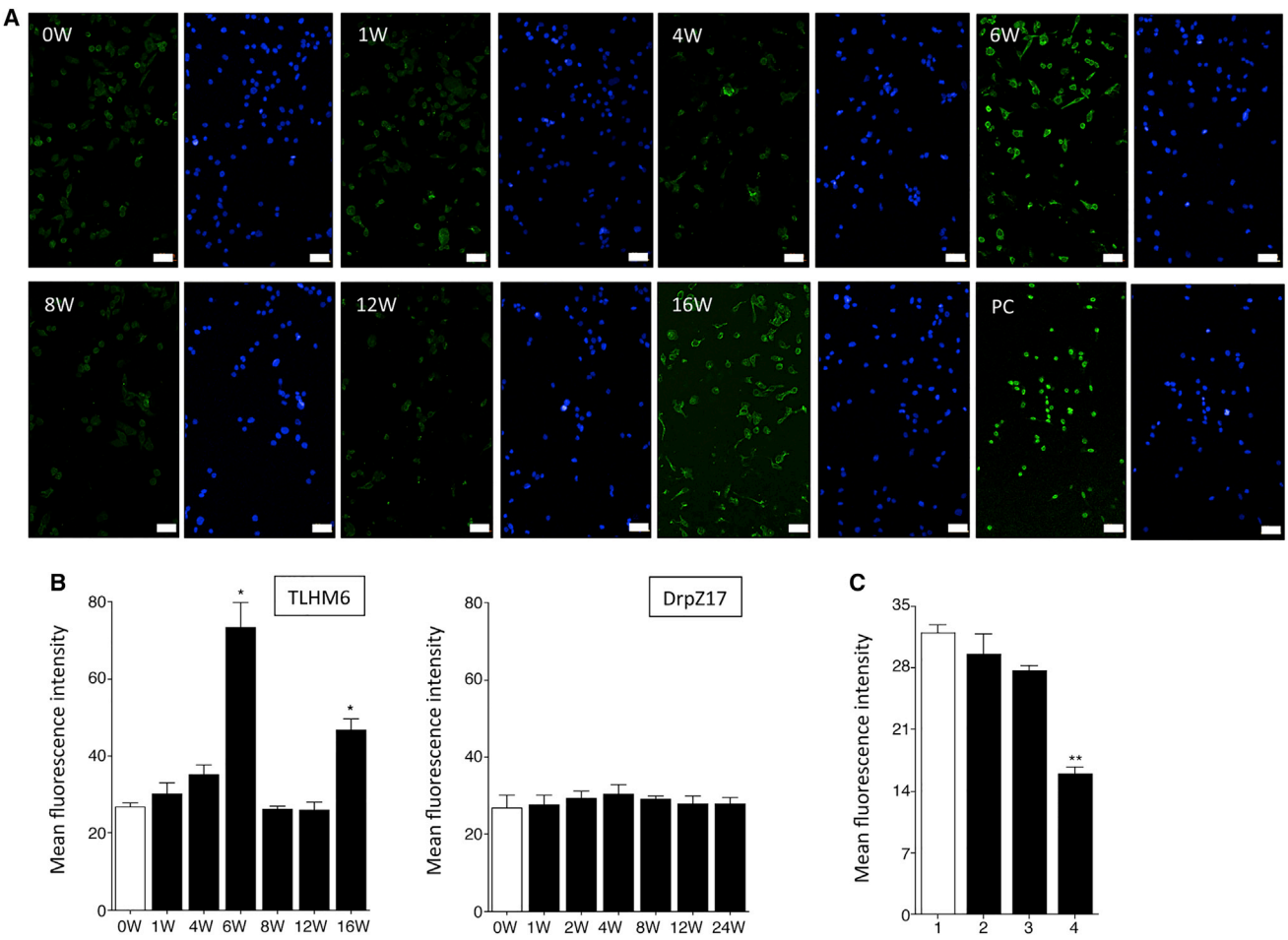

Figure 7. Quantitative Evaluation of RSA Detection in iPS-RPE Cell Transplanted Rejection Monkeys

We regularly collected the serum at 0, 1, 4, 6, 8, 12, and 16 weeks (W) after transplantation in a TLHM6 rejection model.

(A) Immunofluorescence analysis of 46a iPS-RPE cells incubated with the serum from the TLHM6 monkey. Nuclei were counterstained with DAPI (blue). PC, positive control staining. Scale bars, 50 μm.

(B) Quantification of immunofluorescent staining of RPE cells by monkey sera. The mean fluorescence intensity with confocal microscopy obtained by staining with the sera from TLHM6 monkeys is indicated (left panel). The right panel indicates the results of incubation with the sera from a DrpZ17 monkey (collected at 0, 1, 2, 4, 8, 12, and 24 weeks after transplantation) with MHC homozygote iPS-RPE cells (MHC haplotype-matched transplantation). *$p < 0.05$, compared with the control (0 weeks, before transplantation; open bar).

(C) Mean fluorescence intensity with confocal microscopy of staining of 46a iPS-RPE cells by the serum from the TLHM6 rejection monkey that was collected at 6 weeks after transplantation. Before incubation, the 46a iPS-RPE cells were pretreated with mouse IgG (1), anti-MHC-I antibodies (2), anti-MHC-II antibodies (3), or both antibodies (4). **$p < 0.005$, compared with the control (isotype control, open bar). Data are the means ± SEM of three independent experiments.

clonally expand, and differentiate into effector cells, e.g., B cells produce a variety of functionally diverse antibodies. Almost invariably, the initial recognition event occurs in secondary lymphoid organs such as LNs, and alloantigen-specific T and B cell proliferation and differentiation takes place in the LNs. Once generated, alloantigen-specific T and B cells disseminate through the recipient's blood vessels so that they can be delivered to graft sites. As shown in this study, the *in vivo* animal models with allogeneic iPS-RPE cells had T and B cell infiltration in swollen draining LNs, and the collected LN cells could be activated (upregulation of MHC class II and CD86 co-stimulatory molecules on B cells) when co-cultured with the transplanted iPS-RPE cells. These results suggested that donor-specific B cells and alloantibodies are carried via the blood vessels to the site of engraftment where they leave the blood and migrate into the transplanted RPE grafts to recognize the donor alloantigens again.

Rejection that is caused by antibodies is mediated by different mechanisms from rejection that is caused by

T cells, and therefore requires other approaches for the diagnosis of inflammation after transplantation. Recent evidence supports the hypothesis that a subset of cases of rejection might be mediated by alloantibodies (Colvin and Smith, 2005; Lachmann et al., 2006; Terasaki and Ozawa, 2004). Circulating HLA-specific antibodies are common in patients with long-term organ allografts. In a clinical trial (Terasaki and Ozawa, 2004), HLA-specific antibodies were detected in around 20% of patients with renal, heart, liver, or lung allografts. Several investigators have demonstrated that *de novo* antibodies, which first appear after transplantation (the patient is not pre-sensitized), that are specific for graft HLA class I and class II molecules are a risk factor for premature graft loss (Pelletier et al., 2002; Piazza et al., 2001). The graft failure was caused by the *de novo* antibodies and the presence of antibodies preceded graft failure in many renal cases. Therefore, circulating HLA-specific antibodies are typically present months to years before graft dysfunction. Thus, antibody-medicated graft injury might be slow to develop. In this study, we detected RSAs in the sera collected from immune attack monkeys using transplanted iPS-RPE cells as a source of antigen. Moreover, the sera from immune attack monkeys poorly stained the iPS-RPE cells when the RPE cells were pretreated with both anti-MHC class I and class II antibodies, suggesting that the alloantibodies (RSAs) may include HLA (MHC)-specific antibodies. Although transplanted iPS-RPE cells failed to stain with the sera collected at early stages after transplantation, i.e., at 0, 1, or 4 weeks, the RPE cells were stained by the serum that was collected at 6 weeks after transplantation, at which time the monkeys had begun to have immune rejection in the retina. Interestingly, compared with the positive staining of the serum collected at 6 weeks, the serum collected at 8 or 12 weeks failed to stain the RPE cells. However, the RPE cells were clearly stained by the serum collected at 16 weeks, i.e., 2 weeks after the second operation for the left eye. It is assumed that the monkey had acquired donor-specific systemic immunosuppression such as ACAID. Alloantibodies (RSAs) might disappear from the peripheral blood because of such eye-specific systemic immune deviation. In fact, in mouse ACAID models, neonatal RPE cells from C57BL/6 mice established a healthy appearance in the anterior chamber of the BALB/c donor, and the graft was ultimately accepted. Moreover, it was reported that mice bearing allogeneic RPE cells in the anterior chamber displayed ACAID phenomena (Jiang et al., 1994). Importantly, alloantigen insertion into the subretinal space also induced systemic immune deviation (Streilein, 2003). In mouse ACAID models, IgG_2-secreting B cells were selectively suppressed after ACAID induction (Wilbanks and Streilein, 1990). In fact, we detected regulatory T cells ($Foxp3^+$ Treg cells) in the retina from immune rejection primates after iPS-RPE allografting (S.S., unpublished data), suggesting that RPE allografting into the subretinal space might induce Treg cells and systemic immune deviation. However, we have no evidence to support this notion at the moment since there has been no report regarding whether primates and humans have such immune deviation after retinal transplantation. We are currently considering performing ACAID experiments using monkey RPE-related rejection models to address this point.

In conclusion, we detected RPE-specific alloantibodies in immune attack animal models that had B cell invasion in the retina. The timing of B cell invasion into the retina and detection of RSA in the serum of the immune rejection monkey was almost the same. We are therefore currently establishing a protocol using human serum to determine whether we can detect RPE-specific antibodies in the serum of AMD patients (pre- or post-operation). For the diagnosis of immune attacks, the patient's serum should be collected at several time points throughout the follow-up period.

EXPERIMENTAL PROCEDURES

Preparation of Monkey iPS-RPE Cells

We prepared iPSCs from normal cynomolgus monkeys, (1) 1121A1 iPSCs from the HT-1 MHC homozygote monkey, and (2) 46a iPSCs from the Cyn46 MHC heterozygote monkey (Sugita et al., 2016a). The monkey iPSCs and iPS-RPE cells were established from cynomolgus monkeys as previously described (Sugita et al., 2016a). We also prepared human iPS-RPE cells for transplantation (Kamao et al., 2014). The care and maintenance of the monkeys conformed to the ARVO Statement for the Use of Animals in Ophthalmic and Vision Research, and the Use of Laboratory Animals, as well as to the Guidelines of the RIKEN CDB Animal Experiment Committee.

Transplantation of iPS-RPE Cells into the Subretinal Space of Monkeys

Normal control cynomolgus monkeys (*Macaca fascicularis*: TLHM1, TLHM6, TLHM15, S3-2, K-151, K-189, and K-254) were purchased from the Shin Nippon Biomedical Lab., HAMRI Co., and Eve Bioscience Ltd. (Wakayama, Japan), and MHC controlled monkeys (haplotype identical: DrpZ17) were purchased from Ina Research Inc. (Nagano, Japan). For transplantation of iPS-RPE cells/sheets, a complete vitrectomy (Accurus, Alcon) was performed after anesthetization. The iPS-RPE cells/sheets were transplanted into the subretinal space as previously described in detail (Kamao et al., 2014; Sugita et al., 2016a). In order to enhance the inflammation, we pretreated the RPE cells with recombinant interferon gamma (100 ng/mL) for 48 hr before the transplantation. The transplanted cells were monitored by color fundus photographs, FA (both RetCamII and Clarity). and OCT (Nidek) at 1, 2, 4, 8, and 12 weeks and at 6 months after surgery.

Transplantation of an allogeneic monkey 46a iPS-RPE sheet into the subretinal space in a TLHM15 monkey was performed with local immunosuppression using IVTA injection. In vitrectomy, the iPS-RPE sheet was transplanted into the subretinal space, and

triamcinolone acetonide (1 mg/50 μL in vitreous; MaQaid, Wakamoto Pharmaceutical) was subsequently injected into the vitreous space. After 4 weeks, STTA (1 mg/50 μL) was injected into the conjunctival space.

MHC Typing

The results of MHC allele typing in TLHM1, -6, and -15 monkeys are summarized in Table S1. The results of MHC allele typing in S3-2 and DrpZ17 monkeys were described in a previous report (Sugita et al., 2016a). Genotyping of MHC-1 and MHC-II genes in cynomolgus monkeys was performed by pyrosequencing as described (Shiina et al., 2015).

Immunohistochemistry

After monkey sacrifice, monkey eyes that were collected at 4, 8, or 12 weeks or at 6 months were fixed and embedded in paraffin (Sigma-Aldrich). Paraffin-embedded sections were sliced into 10-μm-thick sections in a series of five sequential slides by using an autoslide preparation system (Kurabo). Sections were blocked with 5% goat serum in PBS for 1 hr at room temperature. Primary antibodies against the following antigens were used: IgG (host, rabbit; Abcam, catalog no. ab109489), CD20 (host, rabbit; Abcam, catalog no. ab78237), and CD40 (host, mouse; BioLegend, catalog no. 334304), and the sections were incubated at 4°C overnight. CD3, MHC-II, and Iba1 staining in retinal sections was performed as previously reported (Sugita et al., 2016a). After three rinses with Tween 20 in PBS, the sections were incubated with secondary antibodies for 1 hr at room temperature and counterstained with DAPI (Life Technologies). Images were acquired with a confocal microscope (LSM700, Zeiss). Each retinal layer (anatomy, ganglion cell layer; inner nuclear layer; outer nuclear layer; RPE; and choroid) in the section is shown in Figure S1.

Mixed Lymphocyte Reactions with Monkey iPS-RPE Cells

PBMCs were isolated from healthy or transplanted monkey donors, and allogeneic immune responses were assessed for proliferation by Ki-67 incorporation into the PBMCs. PBMCs were cultured with 46a iPS-RPE cells or allogeneic monkey B cells (EBV-transformed B cells, B95-8) as a positive control. The culture medium used and the detailed methods were previously reported (Sugita et al., 2016a). To avoid RPE cell proliferation during cell culture, we irradiated the RPE cells (20 Gy) before the assay. After 96 hr, the PBMCs were washed and analyzed using flow cytometry (Ki-67 proliferation assay by FACS).

Flow Cytometry

Expression of MHC class II (MHC-II) and CD86 (B7-2) co-stimulatory molecules on B cells in PBMCs was examined by FACS analysis. Before staining, these cells were incubated with an Fc block (Miltenyi Biotec) at 4°C for 15 min. The cells were stained with anti-CD20 (Miltenyi Biotec, catalog no. 130-091-108), anti-MHC-II (anti-human HLA-DP, DQ, DR, Dako, catalog no. Nr.F0817), or anti-CD86 (B7-2, eBioscience, catalog no. 53-0869) antibody or isotype control (mouse IgG) at 4°C for 30 min. PBMCs co-cultured with 46a iPS-RPE cells were also prepared.

For the Ki-67 proliferation assay by FACS analysis (BioLegend), the following antibodies were prepared: APC-labeled anti-CD4 (Miltenyi Biotec, catalog no. 130-091-232), anti-CD8 (eBioscience, catalog no. 17-0088), and anti-CD11b (Miltenyi Biotec, catalog no. 130-091-241); FITC-labeled anti-CD20 (Miltenyi Biotec, catalog no. 130-091-108) and anti-CD56 (BioLegend, catalog no. 304604); and PE-labeled anti-Ki-67 (BioLegend, catalog no. 350504). The harvested PBMCs and the PBMCs co-cultured with iPS-RPE cells were stained with these antibodies at 25°C for 40 min. All antibody information, including isotype controls, is provided in a previous report (Sugita et al., 2016a). All samples were analyzed on a FACSCanto flow cytometer (BD), and data were analyzed using FlowJo software (Tree Star).

Detection of RPE-Specific Antibody

Cultured monkey iPS-RPE cells (46a or 1121A1, 1×10^4 cells/well) were re-cultured in a 96-well culture plate. After removal of the culture supernatants, the RPE cells were fixed with methanol (−30°C) for 15 min at −30°C, washed three times with PBS, and permeabilized with 0.2% Triton X-100 in PBS. Serum samples (TLHM1, TLHM6, TLHM15, S3-2, DrpZ17, and K-151) were collected after surgery. We also prepared iPS-RPE cells that were pretreated with anti-MHC-I (anti-human HLA-ABC, 5 μg/mL, eBioscience, catalog no. 14-9983) antibodies, anti-MHC-II (anti-human HLA-DR, DP, DQ, 5 μg/mL, BD Pharmingen, catalog no. 555557) antibodies, both antibodies (5 μg/mL each), or mouse IgG isotype control (5 μg/mL, eBioscience, catalog no. 14-4724).

Serum (×50 or ×100), anti-human nuclei antibody (positive control, 10 μg/mL, mouse IgG, Millipore, catalog no. MAB1281), anti-VEGF antibody (RPE control, 5 μg/mL, rabbit IgG, Abcam, catalog no. ab52917), and isotype control mouse IgG (negative control, 10 μg/mL, Abcam, catalog no. ab91353) were used as primary antibodies and incubated with the cells at 4°C overnight. The cells were then stained for 1 hr at room temperature with Alexa Fluor 488 anti-human IgG (1 μg/mL, Invitrogen, catalog no. A11013) for the serum samples, Alexa Fluor 488 anti-mouse IgG (1 μg/mL, Invitrogen, catalog no. A11029) for nuclei, or Alexa Fluor 488 anti-rabbit IgG (1 μg/mL, Invitrogen, catalog no. A11034) for VEGF or mouse IgG isotype control staining. Cell nuclei were counterstained with DAPI (5 μg/mL, Invitrogen, catalog no. D1306). We evaluated RSA detection of iPS-RPE cells using a fluorescence microscope (Olympus). At least three independent experiments were performed for IHC analysis. Statistical analyses were performed using Student's t test (paired t test). Values were considered statistically significant if $p < 0.05$.

SUPPLEMENTAL INFORMATION

Supplemental Information includes six figures and one table and can be found with this article online at https://doi.org/10.1016/j.stemcr.2017.10.003.

AUTHOR CONTRIBUTIONS

S.S. was the principal investigator, designed and performed experiments, and wrote the manuscript. K.M. and S.F. evaluated ocular findings after transplantation. Y.I. collected LN tissues. H.K. performed the transplantation. T.S. and K.O. performed monkey

MHC analysis. M.T. designed and conceptualized the study and drafted and edited the manuscript.

ACKNOWLEDGMENTS

We thank N. Hayashi, K. Iseki, T. Hashiguchi, M. Kawahara, and C. Yamada (Laboratory for Retinal Regeneration, Center for Developmental Biology, RIKEN, Kobe, Japan) for their expert technical assistance. We thank Prof. J. Hamuro (Department of Ophthalmology, Kyoto Prefectural University of Medicine, Kyoto, Japan) for technical advice. We thank Drs. Y. Hirami and Y. Kurimoto (Department of Ophthalmology, Institute of Biomedical Research and Innovation Hospital, Kobe, Japan) for the transplantation of monkey iPS-RPE cells. This work was supported by a Scientific Research Grant (B, 25293357) from the Ministry of Education, Culture, Sports, Science and Technology of Japan and by the Research Center Network for Realization of Regenerative Medicine from the Japan Agency for Medical Research and Development (AMED).

Received: July 27, 2017
Revised: October 5, 2017
Accepted: October 5, 2017
Published: November 2, 2017

REFERENCES

Algvere, P.V. (1997). Clinical possibilities in retinal pigment epithelial transplantations. Acta Ophthalmol. Scand. *75*, 1.

Algvere, P.V., Gouras, P., and Dafgard Kopp, E. (1999). Long-term outcome of RPE allografts in non-immunosuppressed patients with AMD. Eur. J. Ophthalmol. *9*, 217–230.

Berry, G.J., Burke, M.M., Andersen, C., Bruneval, P., Fedrigo, M., Fishbein, M.C., Goddard, M., Hammond, E.H., Leone, O., Marboe, C., et al. (2013). The 2013 International Society for Heart and Lung Transplantation Working Formulation for the standardization of nomenclature in the pathologic diagnosis of antibody-mediated rejection in heart transplantation. J. Heart Lung Transplant. *32*, 1147–1162.

Colvin, R.B., and Smith, R.N. (2005). Antibody-mediated organ-allograft rejection. Nat. Rev. Immunol. *5*, 807–817.

Goslings, W.R., Yamada, J., Dana, M.R., Streilein, J.W., van Beelen, E., Prodeus, A.P., Carroll, M.C., and Jager, M.J. (1999). Corneal transplantation in antibody-deficient hosts. Invest. Ophthalmol. Vis. Sci. *40*, 250–253.

Hegde, S., Mellon, J.K., Hargrave, S.L., and Niederkorn, J.Y. (2002). Effect of alloantibodies on corneal allograft survival. Invest. Ophthalmol. Vis. Sci. *43*, 1012–1018.

Jiang, L.Q., Jorquera, M., and Streilein, J.W. (1994). Immunologic consequences of intraocular implantation of retinal pigment epithelial allografts. Exp. Eye Res. *58*, 719–728.

Kamao, H., Mandai, M., Okamoto, S., Sakai, N., Suga, A., Sugita, S., Kiryu, J., and Takahashi, M. (2014). Characterization of human induced pluripotent stem cell-derived retinal pigment epithelium cell sheets aiming for clinical application. Stem Cell Reports *2*, 205–218.

Lachmann, N., Terasaki, P.I., and Schonemann, C. (2006). Donor-specific HLA antibodies in chronic renal allograft rejection: a prospective trial with a four-year follow-up. Clin. Transpl., 171–199.

Mandai, M., Watanabe, A., Kurimoto, Y., Hirami, Y., Morinaga, C., Daimon, T., Fujihara, M., Akimaru, H., Sakai, N., Shibata, Y., et al. (2017). Autologous induced stem-cell-derived retinal cells for macular degeneration. N. Engl. J. Med. *376*, 1038–1046.

Mochizuki, M., Sugita, S., and Kamoi, K. (2013). Immunological homeostasis of the eye. Prog. Retin. Eye Res. *33*, 10–27.

Pelletier, R.P., Hennessy, P.K., Adams, P.W., and Orosz, C.G. (2002). High incidence of donor-reactive delayed-type hypersensitivity reactivity in transplant patients. Am. J. Transplant. *2*, 926–933.

Piazza, A., Poggi, E., Borrelli, L., Servetti, S., Monaco, P.I., Buonomo, O., Valeri, M., Torlone, N., Adorno, D., and Casciani, C.U. (2001). Impact of donor-specific antibodies on chronic rejection occurrence and graft loss in renal transplantation: posttransplant analysis using flow cytometric techniques. Transplantation *71*, 1106–1112.

Sheng, Y., Gouras, P., Cao, H., Berglin, L., Kjeldbye, H., Lopez, R., and Rosskothen, H. (1995). Patch transplants of human fetal retinal pigment epithelium in rabbit and monkey retina. Invest. Ophthalmol. Vis. Sci. *36*, 381–390.

Shiina, T., Yamada, Y., Aarnink, A., Suzuki, S., Masuya, A., Ito, S., Ido, D., Yamanaka, H., Iwatani, C., Tsuchiya, H., et al. (2015). Discovery of novel MHC-class I alleles and haplotypes in Filipino cynomolgus macaques (*Macaca fascicularis*) by pyrosequencing and Sanger sequencing: Mafa-class I polymorphism. Immunogenetics *67*, 563–578.

Streilein, J.W. (2003). Ocular immune privilege: therapeutic opportunities from an experiment of nature. Nat. Rev. Immunol. *3*, 879–889.

Streilein, J.W., Ma, N., Wenkel, H., Ng, T.F., and Zamiri, P. (2002). Immunobiology and privilege of neuronal retina and pigment epithelium transplants. Vision Res. *42*, 487–495.

Sugita, S. (2009). Role of ocular pigment epithelial cells in immune privilege. Arch. Immunol. Ther. Exp. (Warsz) *57*, 263–268.

Sugita, S., Iwasaki, Y., Makabe, K., Kamao, H., Mandai, M., Shiina, T., Ogasawara, K., Hirami, Y., Kurimoto, Y., and Takahashi, M. (2016a). Successful transplantation of retinal pigment epithelial cells from MHC homozygote iPSCs in MHC-matched models. Stem Cell Reports *7*, 635–648.

Sugita, S., Iwasaki, Y., Makabe, K., Kimura, T., Futagami, T., Suegami, S., and Takahashi, M. (2016b). Lack of T Cell response to iPSC-derived retinal pigment epithelial cells from HLA homozygous donors. Stem Cell Reports *7*, 619–634.

Terasaki, P.I., and Ozawa, M. (2004). Predicting kidney graft failure by HLA antibodies: a prospective trial. Am. J. Transplant. *4*, 438–443.

van Meurs, J.C., ter Averst, E., Hofland, L.J., van Hagen, P.M., Mooy, C.M., Baarsma, G.S., Kuijpers, R.W., Boks, T., and Stalmans, P. (2004). Autologous peripheral retinal pigment epithelium translocation in patients with subfoveal neovascular membranes. Br. J. Ophthalmol. *88*, 110–113.

Wallace, W.D., Weigt, S.S., and Farver, C.F. (2014). Update on pathology of antibody-mediated rejection in the lung allograft. Curr. Opin. Organ Transplant. *19*, 303–308.

Weisz, J.M., Humayun, M.S., De Juan, E., Jr., Del Cerro, M., Sunness, J.S., Dagnelie, G., Soylu, M., Rizzo, L., and Nussenblatt, R.B. (1999). Allogenic fetal retinal pigment epithelial cell transplant in a patient with geographic atrophy. Retina *19*, 540–545.

Wilbanks, G.A., and Streilein, J.W. (1990). Distinctive humoral immune responses following anterior chamber and intravenous administration of soluble antigen. Evidence for active suppression of IgG2-secreting B lymphocytes. Immunology *71*, 566–572.

Stem Cell Reports, Volume *9*

Supplemental Information

Detection of Retinal Pigment Epithelium-Specific Antibody in iPSC-Derived Retinal Pigment Epithelium Transplantation Models

Sunao Sugita, Kenichi Makabe, Shota Fujii, Yuko Iwasaki, Hiroyuki Kamao, Takashi Shiina, Kazumasa Ogasawara, and Masayo Takahashi

Supplementary Figure 1.

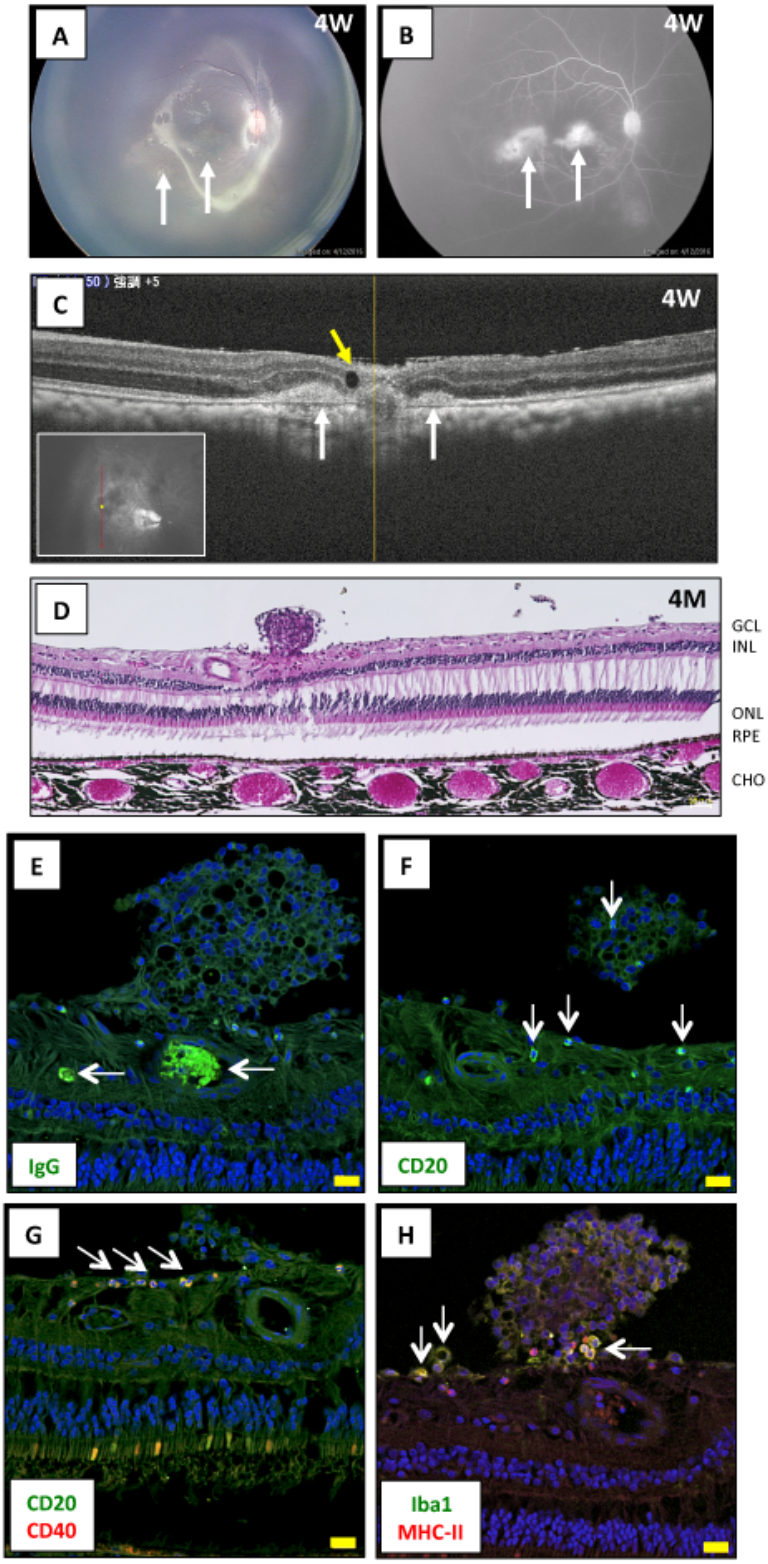

Allogeneic transplantation of iPSC-derived RPE cells into the subretinal space of a monkey and B cell related immunostaining. Transplantation of monkey 46a iPS-RPE sheets (two sheets into the right

eye) into the subretinal space in a TLHM6 normal monkey was performed without immunosuppression. Fibroblastic scar-like sheets in a fundus photograph (**A,** arrows) and leakage from the graft sheets in fluorescein angiography (FA; **B,** arrows) were observed at the 4-week (4W) evaluation. Optical coherence tomography (OCT; **C**) revealed the presence of retinal cystic edema (yellow arrow) and retinal infiltration (white arrows) in the subretinal space. (**D**) Hematoxylin-eosin (HE)-stained section of the TLHM6 monkey eye [section at 4 months (4M) after transplantation] for histological interpretation. There was an inflammatory nodule on the retina. GCL, ganglion cell layer; INL, inner nuclear layer; ONL, outer nuclear layer; RPE, retinal pigment epithelium; CHO, choroid. Scale bar, 50 μm. (**E-H**) Photomicrographs showing labeling of the retina in the right eye of a TLHM6 monkey with anti-IgG, CD20/CD40, and MHC class II (MHC-II) antibodies using retinal sections. In the eye, there was enhanced IgG staining in the retina (**E,** white arrows) under the mass of the retinal nodules. Numerous $CD20^+$ cells (**F,** white arrows) and $CD20^+/CD40^+$ double-positive cells (**G**, white arrows) were observed in the retina. In addition, we found $Iba1^+/MHC\text{-}II^+$ double-positive cells (antigen-presenting cells) around the retinal nodules (**H,** white arrows). Scale bars, 20 μm.

Supplementary Figure 2.

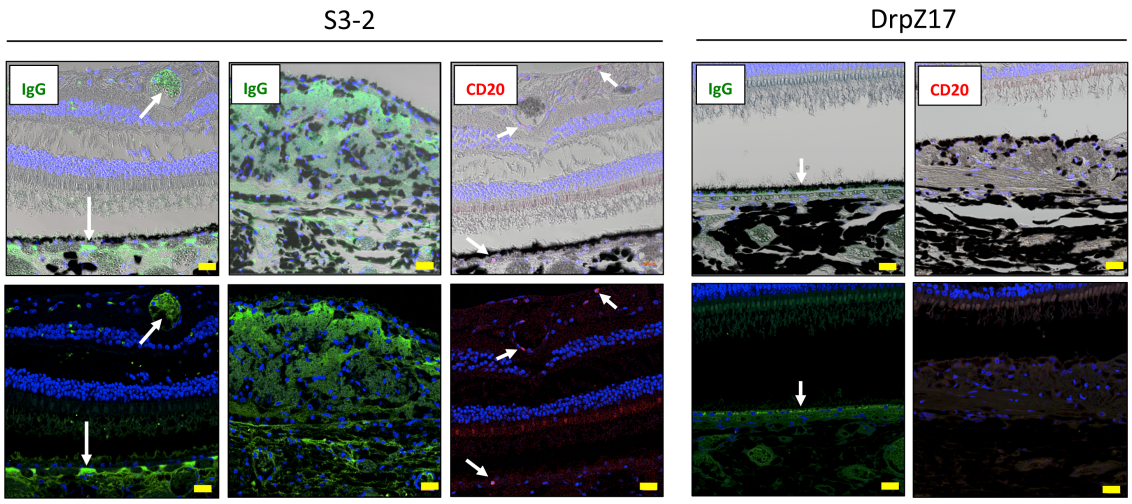

B cell related immunohistochemistry in monkeys that received allogeneic transplantation of iPSC-derived RPE cells: an MHC haplotype-mismatched monkey (S3-2) and an MHC haplotype-matched monkey (DrpZ17). Photomicrographs showing labeling of the retina in the left eye of an S3-2 or DrpZ17 monkey with anti-IgG or CD20 antibodies using paraffin-embedded sections. In the S3-2 eye, there was enhanced IgG staining in the retina and under the host RPE layer (left images, white arrows) as well as in the mass of the retinal nodules (middle images). In addition, numerous $CD20^{+}$ cells in the retina and RPE layer (right images, white arrows) were observed. Conversely, in the DrpZ17 monkey (MHC haplotype-matched allograft; 1121A1 MHC homozygote iPS-RPE sheets → DrpZ17 MHC control monkey), weak IgG staining (left images, white arrow) was seen in the RPE layer. The iPS-RPE cell sheet seemed to be intact with no infiltration of $CD20^{+}$ B cells into the DrpZ17 monkey eye (right images). Scale bars, 20 μm.

Supplementary Figure 3.

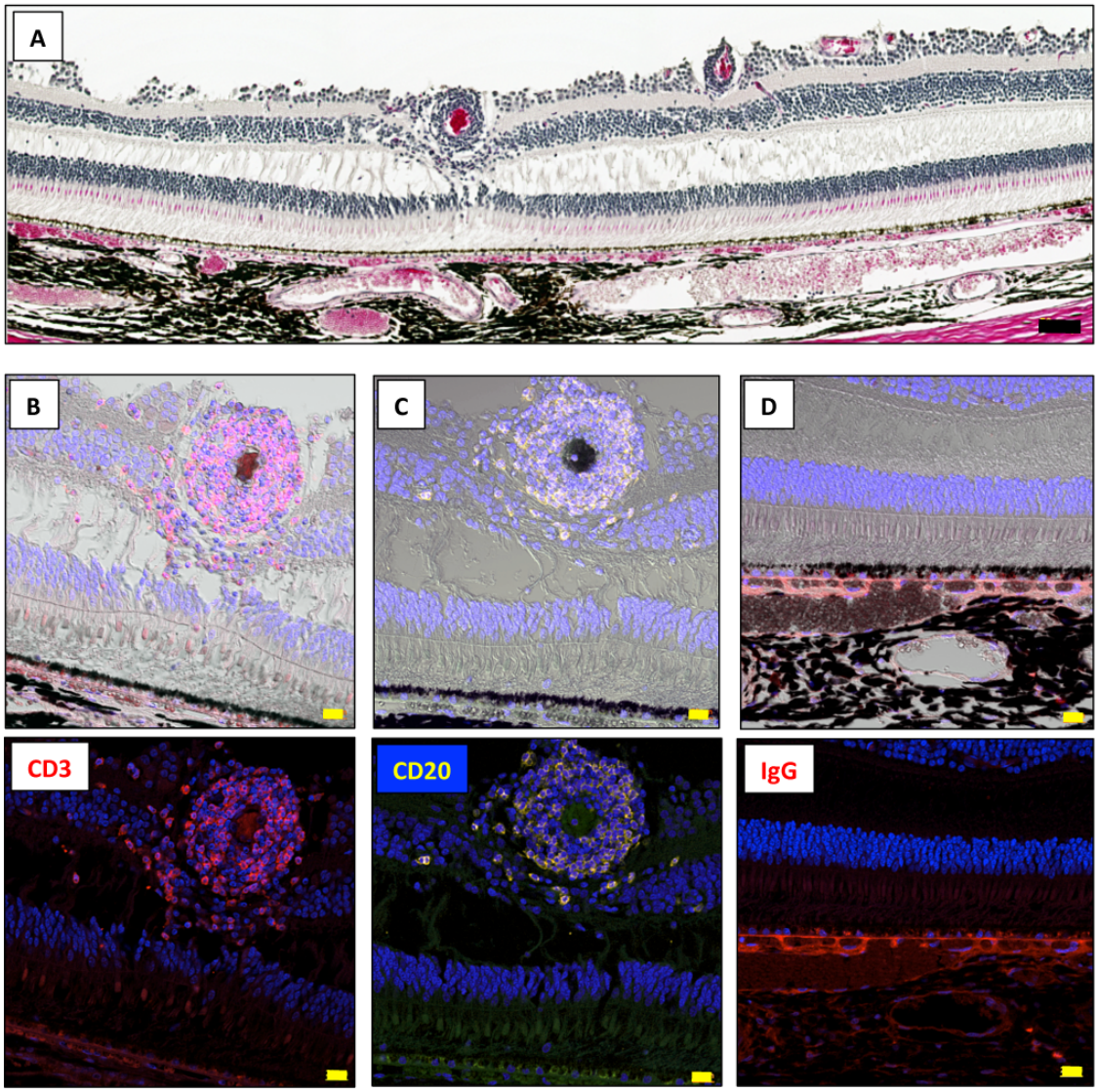

Transplantation of human iPSC-derived RPE cells (xenografts) into the subretinal space of a monkey and B/T cell related immunostaining. We prepared a human iPS-RPE cell suspension (MTEV19 cells: 5×10^4 cells) for the transplantation. (**A**) Hematoxylin-eosin-stained section of the K-189 monkey right eye (section at 6 months after transplantation) for histological interpretation. There was an inflammatory nodule on the retina. Photomicrographs showing labeling of the retina in the right eye of the monkey with anti-CD3 (**B**), anti-CD20 (**C**), or anti-IgG antibody (**D**) using paraffin-embedded sections. In the eye, numerous $CD3^+$ T cells (left image) and $CD20^+$ B cells (middle image) were observed in the mass of the retinal nodules. In addition, there was enhanced IgG staining under the host RPE layer (left image). Scale bars, 20 μm.

Supplementary Figure 4.

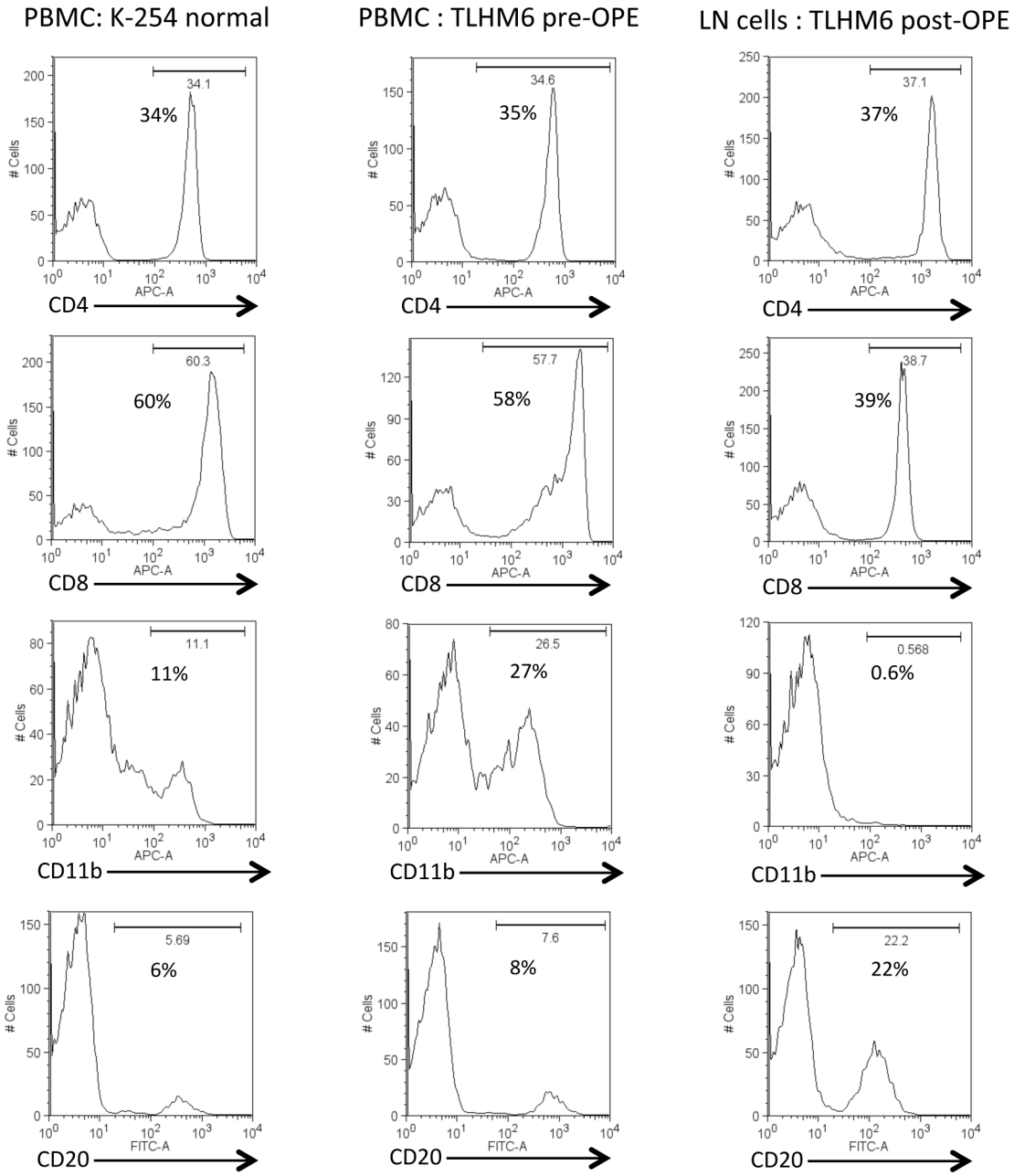

Detection of B cells in PBMCs or lymph nodes from a monkey with immune rejection. PBMCs were collected from a normal control monkey (K-254) and a TLHM6 monkey (pre-operation, pre-OPE) in order to evaluate the percentage of B cells in the periphery. Lymph node (LN) cells were also collected from the TLHM6 monkey after transplantation (4 months post-OPE). Briefly, PBMCs or LN cells were stained with anti-CD4, anti-CD8, anti-CD11b, anti-CD20, and each isotype control antibody at 4°C for 30 min and these cells were then analyzed on a FACS flow cytometer. Numbers (%) in the histograms indicate the percentage of cells positive for the indicated antigen.

Supplementary Figure 5.

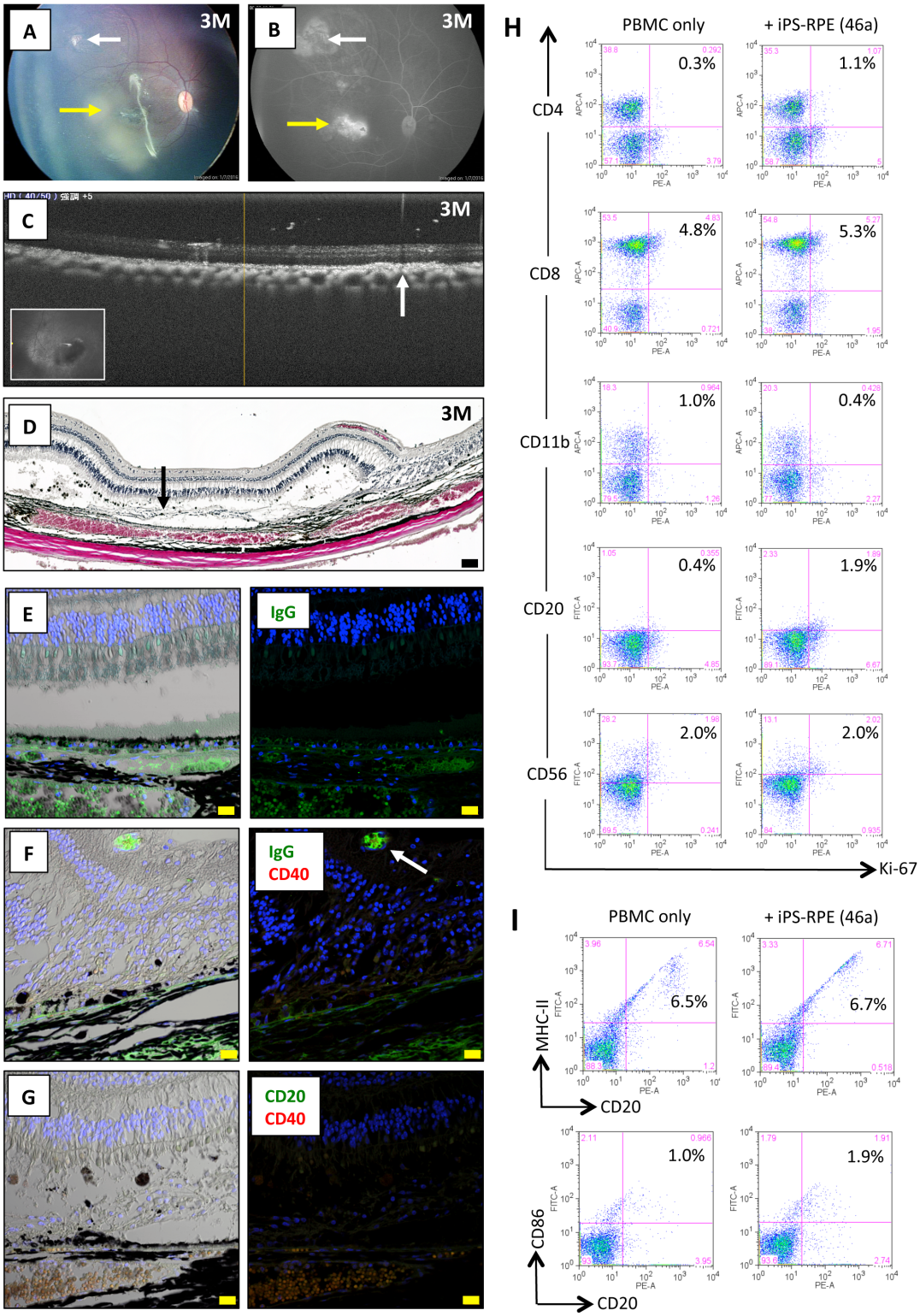

Allogeneic transplantation of an iPS-RPE cell sheet into the subretinal space of a monkey with local steroid injection and B cell related immunohistochemistry. Transplantation of a 46a iPS-RPE sheet (right eye) into the subretinal space in a TLHM15 monkey was performed with local immunosuppression

by IVTA/STTA injection. (**A**) In the operated right eye [3-month (3M) evaluation], the transplanted RPE sheet (white arrow) is shown in a fundus photograph. The yellow arrow indicates macular damage due to operation error. (**B**) No leakage from the graft sheet was observed in fluorescein angiography (**A,** arrows), and (**C**) OCT evaluation showed a graft sheet without inflammatory signs. (**D**) Hematoxylin-eosin analysis at 3M showed the RPE sheet with few inflammatory cells in the subretinal space. Scale bar, 50 μm. (**E-G**) Photomicrographs showing labeling of the TLHM15 monkey retina with anti-IgG, anti-CD20, or anti-CD40 antibody. Little IgG staining (**E, F**), and no $CD20^+$ or $CD40^+$ cells (**F, G**) were seen in paraffin-embedded sections of the retina. Scale bars, 20 μm. (**H**) MLR assay using PBMCs from the TLHM15 monkey and transplanted iPS-RPE cells. In the PBMC-RPE MLR assay *in vitro*, $CD4^+$/Ki-67^+ (proliferated helper T cells), $CD8^+$/Ki-67^+ (proliferated cytotoxic T cells), $CD11b^+$/Ki-67^+ (proliferated monocytes), $CD20^+$/Ki-67^+ (proliferated B cells), and $CD56^+$/Ki-67^+ (proliferated NK/NKT cells) cells were evaluated using flow cytometry. Compared with PBMCs only, all types of PBMCs that were exposed to transplanted 46a iPS-RPE cells were poorly proliferated. Numbers (%) in the histogram indicate double-positive cells (e.g., $CD4^+$/Ki-67^+). (**I**) Expression of MHC-II and CD86 molecules on B cells exposed to iPS-RPE cells. PBMCs in the presence of iPS-RPE cells were stained with anti-MHC-II, anti-CD86, and ani-CD20 antibodies. Compared with PBMCs only, expression of these molecules on $CD20^+$ B cells in PBMCs exposed to 46a iPS-RPE cells was almost the same, suggesting that PBMCs from the TLHM15 monkey do not include activated memory B cells. Numbers (%) in the histogram indicate double-positive cells (e.g., $CD20^+$/MHC-II^+).

Supplementary Figure 6.

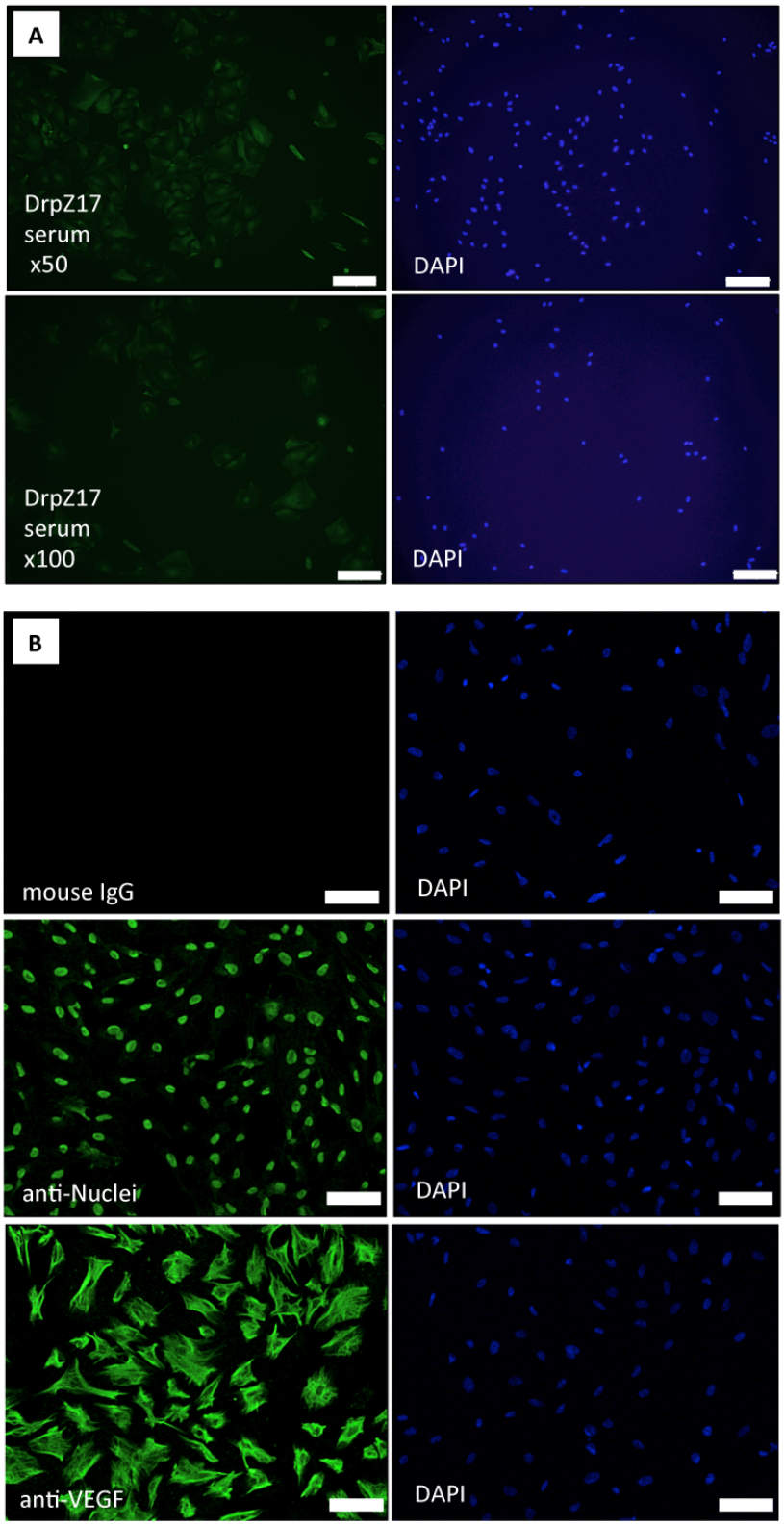

Detection of RPE-specific antibody (RSA) in the iPSC-derived RPE transplanted animal model with MHC haplotype-matched identity. Serum was collected from the operated MHC

haplotype-matched monkey, DrpZ17, at 12 weeks after surgery, and transplanted iPS-RPE cells (1121A1 MHC homozygote lines) were prepared. After RPE cell fixation, immunohistochemistry was performed using the diluted serum for RSA detection. (**A**) iPS-RPE cells + serum from the DrpZ17 monkey, (**B**) negative control staining (mouse IgG: upper image); anti-nuclei, positive control staining (middle image); anti-VEGF, RPE control staining (lower image). DAPI, nuclear staining (blue). Scale bars, 200 μm.

Supplementary Table 1.

Supplementary Table 1. Results of MHC allele typing in transplanted monkeys

MHC antigens	Name	TLHM1 monkey	TLHM6 monkey	TLHM15 monkey
	DOB	4/3/2010	5/19/2009	2/26/2008
	Age	6 Y	7 Y	8 Y
	Country	Japan	China	China
	Sex	Male	Male	Male
Mafa class I (MHC class I)	Mafa-A1	A1*015:01/02/03	A1*032:04 A1*065:04:02	A1*022:01
	Mafa-A2-A5	A4*14:01/08/10_new	A3*13:07 A4*14:03/04	A4*14:03/04
	Mafa-B sub-region	B*007:01 B*039:01 B*050:02 B*060:04 B*064:03_new B*065:02 B*069:03_new B*117:01/02_new B*148:01_new	B*041:01 B*060:02 B*065:02 B*069:03 B*072:03_new B*095:01 B*101:01 B*104:03 B*154:01 B*155:01	B*013:04_new B*013:06_new B*013:10 B*014:01 B*036:01 B*037:01_new B*041:01_new B*045:03_new B*050:02 B*072:03_new B*115:04:02_new
Mafa class II (MHC class II)	Mafa-DRB sub-region	DRB3*04:03 DRB*W4:04 DRB*W20:03 DRB*W25:01 DRB*W27:04	DRB*W37:01 DRB*W49:01 DRB1*04:13 DRB1*10:02	DRB*W1:01 DRB*W3:02 DRB1*03:03/30 DRB1*04:02 DRB1*W4:01
	Mafa-DQA1	DQA1*23:01_new DQA1*24:04	DQA1*05:03_new DQA1*05:04	DQA1*01:03 DQA1*01:04
	Mafa-DQB1	DQB1*18:04 DQB1*18:16/21	DQB1*16:01 DQB1*17:05	DQB1*06:01 DQB1*06:16
	Mafa-DPA1	DPA1*10:01	DPA1*02:06/08_new DPA1*10:01	DPA1*02:20_new DPA1*10:01_new
	Mafa-DPB1	DPB1*18:01 DPB1*18:02	DPB1*07:01 DPB1*18:02	DPB1*15:05 DPB1*18:01
Grafts (right eye / left eye)		46a iPS-RPE sheets/ sheets	46a iPS-RPE sheets/-	46a iPS-RPE sheets/-
MHC matched to 46a iPS-RPE cells		No	No	No
Immune rejection (right eye / left eye)		Yes / Yes	Yes /-	No /-
Medication (right eye / left eye)		None	None	IVTA/STTA injection /-
Obsevation period (right eye / left eye)		6M / 4W	4M /-	3M /-

New in MHC results indicates new allele gene. IVTA - intravitreal triamcinolone acetonide. STTA - sub-Tenon triamcinolone acetonide.